Univerzita Karlova v Praze

Přírodovědecká fakulta

Studijní program: Biologie

Studijní obor: Buněčná a vývojová biologie

Bc. Kateřina Škarabellová

Studies towards biological function of ubiquitin E3 ligase RNF121 *in vivo* and *in vitro*

Studie vztahující se k biologické funkci ubiquitin E3 ligázy RNF121 *in vivo* a *in vitro*

Diplomová práce

Vedoucí diplomové práce: Doc. Radislav Sedláček, PhD.

Konzultant diplomové práce: Silvia Petrezsélyová, PhD.

Praha, 2016

Prohlášení

Prohlašuji, že jsem závěrečnou práci zpracovala samostatně a za použití níže citovaných literárních zdrojů. Tato práce ani její podstatná část nebyla předložena k získání jiného nebo stejného akademického titulu.

V Praze Bc. Kateřina Škarabellová

Acknowledgements

I would like to thank many people who contributed to this diploma thesis. Firstly, many thanks to my supervisor Doc. Radislav Sedláček, PhD. for his advices and giving me the opportunity to work on interesting project in the Department of Transgenic Models of Diseases. I would like to thank to my consultant, Silvia Petrezsélyová, Ph.D, for her patience, support, numerous advices and consultations during the diploma thesis. My thanks go also to Kallayanee Chawengsaksophak, Ph.D., for her valuable advices in the field of embryology.

Beside this, I am very greatfull to my colleagues Barbora Singerová, Shohag Bhattacharyya, Věra Mihálová, Veronika Grešáková, Slavomír Kinský, Iris Manosalva and other people from our lab for their helpfull advices.

Last but not least, I would like to thank to my family for all the support they gave me.

Abstract

Although the RING finger protein 121 (RNF121) is a highly conserved E3 ubiquitin ligase from *Caenorhabditis elegans* to human, its function is poorly understood and in higher eukaryotes it has been studied only at *in vitro* level. RNF121 has been described to have various functions: i) it was ascribed to function as a broad regulator of NF-κB activation, ii) it was shown to control intracellular trafficking of various membrane proteins, and iii) its downregulation leads to apoptosis. Moreover, RNF121 might have a role in cancer as its expression was found to be 16.4-fold higher in patients suffering from Barrett esophagus (precancerous lesion of esophageal adenocarcinoma) and was even more increased in esophageal adenocarcinoma comparing to healthy population. In addition, *RNF121* gene is localized in the candidate region containing breast cancer susceptibility genes.

To gain insight into physiological functions of RNF121, *Rnf121* knockout mice (*Rnf121*$^{tm1b(EUCOMM)Hmgu}$) were generated in the Czech Centre for Phenogenomics and further studied in our laboratory. *Rnf121*$^{+/-}$ intercross breedings showed a prenatal lethal phenotype of *Rnf121*$^{-/-}$embryos, which were dying prior embryonic day (E) 11.5. Preliminary experiments carried out in our laboratory showed numerous vascular defects in null mutant embryo, yolk sac and placenta. This diploma thesis aimed to investigate function of murine RNF121 in the embryonic development with focus on the placenta forming and vascularization. It was found out that RNF121 plays an important role in placenta development since in *Rnf121*$^{-/-}$ placenta smaller trophoblast and underdeveloped labyrinth were observed. Besides this, it was confirmed that RNF121 participates in the activation of the NF-κB pathway on *Rnf121*$^{-/-}$ mouse embryonic fibroblasts.

Key words: E3 ligase, ubiquitin, ring-finger, NF-κB, mouse knockout, placenta, vascularization

Abstrakt

Přestože je RING finger protein 121 (RNF121) vysoce konzervovaná E3 ubiquitin ligáza, a to od *Caenorhabditis elegans* k člověku, její funkce není moc známá a u vyšších eukaryot byla zatím studována jen na úrovni *in vitro*. Pro RNF121 byly popsány různé funkce: i) RNF121 funguje jako široký regulátor NF-κB aktivace, ii) ukázalo se, že kontroluje transport membránových proteinů uvnitř buňky, a iii) jeho downregulace vede k apoptóze. Kromě toho může mít RNF121 roli také při rakovině a to na základě nasledovních dat: 16.4-krát vyšší exprese byla zjištěna u pacientů trpících Barrettovým jícnem (prekancerózním stádiem adenokarcinomu jícnu) a tato exprese byla ještě vyšší u adenokarcinomu v porovnání se zdravou populací. Navíc je *RNF121* gen lokalizován v kandidátní oblasti DNA obsahující geny, které se mohou účastnit vzniku rakoviny prsu.

Za účelem studia fyziologické funkce RNF121, byl v Českém centru pro fenogenomiku připraven myší *Rnf121* knockout, který byl dále studovaný v naší laboratoři. Křížení $Rnf121^{+/-}$ myší poukázalo na prenatální letální fenotyp $Rnf121^{-/-}$ embryí, která odumírala před embryonálním dnem (E) 11.5. Předběžné experimenty provedené v naší laboratoři prokázaly četné vaskulární defekty v homozygotně mutantním embryu, ve žloutkovém vaku a v placentě. Tato diplomová práce byla zaměřena na studium funkce myšího RNF121 v embryonálním vývoji se zaměřením na utváření placenty a vaskularizaci. Bylo zjištěno, že RNF121 hraje důležitou roli v placentálním vývoji, jelikož byl v $Rnf121^{-/-}$ placentě pozorován menší trofoblast a nedostatečně vyvinutý labyrint. Kromě toho bylo na $Rnf121^{-/-}$ myších embryonálních fibroblastech potvrzeno, že RNF121 se účastní aktivace NF-κB dráhy.

Klíčová slova: E3 ligáza, ubiquitin, ring-finger, NF-κB, myší knockout, placenta, vaskularizace

Contents

List of abbreviations

Ang-1	angiopoietin-1
APC	anaphase promoting complex
ASCR	Academy of Sciences of the Czech Republic
BAFF	β-cell activating factor
BARD1	BRCA1-associated RING domain 1
bp	base pairs
BRCA1	breast cancer 1
BSA	bovine serum albumin
Cdc20	cell division cycle 20
CHD	cullin homology domain
cIAP	cellular inhibitor of apoptosis
CRL	cullin RING ligase
CUL	cullin
DEPC	diethylpyrocarbonate
DIG	digoxigenin
DMEM	Dulbeccos´s Modified Eagle Medium
dNTPs	deoxyribonucleotides
DUBs	deubiquitinases
E	embryonic stage
E1	ubiquitin-activating enzmye
E2	ubiquitin-conjugating enzyme
E3	ubiquitin-ligating enzyme
Egf	epidermal growth factor
ER	endoplasmic reticulum
FANC	Fanconi anemia complementation group

Fgf	fibroblast growth factor
GC	glycogen trophoblast cell
GFP	green fluorescent protein
HECT	homology to the E6-AP carboxyl terminus
HIF-1	hypoxia inducible factor 1
ICM	inner cell mass
IKK	IκB kinase
IL-1β	interleukin 1β
IMG	Institute of Molecular Genetics
IMPC	International Mouse Phenotyping Consortium
IκB	inhibitor of κB
kDa	kilo Daltons
Lab	labyrinthe
MD	maternal decidua
MDM2	murine double minute 2
MDMX	murine double minute X
MEF	mouse embryonic fibroblast
Na_V	voltage-gated sodium channel
NEMO	NF-κB essential modulator
NF-κB	nuclear factor κB
NLS	nuclear localization signal
PAGE	polyacrylamide gel electrophoresis
PARC	p53-associated parkin-like cytoplasmic protein
PARP	poly (ADP-ribose) polymerase
PCR	polymerase chain reaction
PDGFβ	plateled-derived growth factor β
PFA	paraformaldehyde
RBR	RING between RING

RBX1	RING box protein 1
RHD	REL homology domain
RING	really interesting new gene
RNF	RING finger
SCF	SKP, Cullin, F-box
SDS	sodium dodecylsulfate
SKP1	S-phase kinase-associated protein 1
TAK1	transforming growth factor-β-activated kinase
TGC	trophoblast giant cell
TLR	Toll-like receptor
TNF-α	tumor necrosis factor α
TRAF	TNF receptor associated factor
Ub	ubiquitin
VE cadherin	vascular endothelial cadherin
VEGF	vascular endothelial growth factor
VEGFR-2	vascular endothelial growth factor receptor 2
Wt	wild-type
β-TrCP	β transducin repeat-containing protein

1. Introduction

The attachment of ubiquitin to intracellular protein, a process called ubiquitination, plays a key role in many cellular processes. Although this post-translational modification is best known for targeting proteins for degradation by the 26S proteasome, ubiquitination mediates a variety of non-proteolytic functions such as alteration of intracellular trafficking, modulation of protein functions and their interactions, and regulation of transcription or DNA repair. The E3 ubiquitin ligases (E3s) are enzymes which bring the substrate specificity into the reaction. In mammals, there are three main ligase families, but the vast majority of E3s belongs to the Really Interesting New Gene (RING) E3 ligase family. RING E3s play numerous essential roles in physiology and pathophysiology, mutations within them are often associated with a variety of human diseases, including cancer. Of over 600 mammalian RING domain-containing genes, only a small number has been studied so far and so, the biological function of most of them remains unknown.

One of the recently described RING E3 ligase is RNF121, which is a highly conserved protein from *C. elegans* to humans. In spite of that fact, its function is poorly described and in higher eukaryotes at *in vitro* level only. RNF121 was first described in the nematode as an endoplasmic reticulum localized protein, in humans it was shown to be predominantly a Golgi-resident protein. RNF121 has been described to have various functions. It was ascribed to function as a broad regulator of NF-κB activation, its downregulation triggers the apoptosis and it was shown to control intracellular trafficking of various membrane proteins. Moreover, epidemiology studies imply that RNF121 might be linked to various types of human cancer.

Within the International Mouse Phenotype Consortium (IMPC), *Rnf121* knockout mice (*Rnf121*$^{tm1b(EUCOMM)Hmgu}$) were generated in the Czech Centre for Phenogenomics. *Rnf121*$^{+/-}$ intercross breedings showed a prenatal lethal phenotype of *Rnf121*$^{-/-}$ embryos which were dying prior to embryonic day (E) 11.5. Examination of earlier embryonic stages (E9.5 – 10.5) revealed severe vascular defects in embryo, yolk sac and placenta (Kallayanee Chawengsaksophak, Ph.D, IMG; unpublished).

Proper development of the placenta and its blood vessels forming are together with the embryonic vascular development essential for survival of the fetus during gestation. Therefore, further specification of the RNF121 role *in vivo,* especially in the placental development was the subject of this diploma thesis. Regarding *in vitro* experiments, the aim was to confirm the participation of RNF121 in the NF-κB pathway using mouse *Rnf121*$^{-/-}$ knockout model. In an attempt to better understand the role of RNF121 at molecular level, a substrate detection assay was performed.

2. Literature review

2.1. Ubiquitination and ubiquitin E3 ligases

The ubiquitination is a post-translational modification which plays a key role in many cellular processes. Proteins responsible for the specificity of this mechanism are called E3 ubiquitin ligases. These ligases recognize target substrates and then mediate the transfer of ubiquitin (Ub), a 76-amino-acid polypeptide (Fig. 1), from the E2 ubiquitin conjugating enzyme to the substrate. The process of ubiquitination was discovered in 1980s by Aaron Ciechanover, Avram Hershko and Irwin Rose I. (Ciechanover *et al*., 1980; Hershko e*t al*., 1980), and it was awarded by the Nobel Prize in Chemistry in 2004.

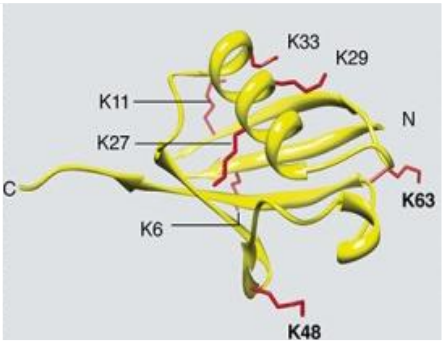

Figure 1: Structure of ubiquitin
The ubiquitin molecule consists of 76 amino-acids and can bind to substrates via seven lysine residues – K6, K11, K27, K29, K33, K48 and K63 and via a free N-terminus (Metzger *et al*., 2012).

Ubiquitination can be characterized as post-translational covalent attachment of ubiquitin to substrates. This process is best known for targeting proteins for degradation by the 26S proteasome. But, there are also other functions of ubiquitination, including lysosomal targeting, modulation of protein functions and their interactions, alteration of subcellular distribution, regulation of transcription or DNA repair and propagation of transmembrane signaling, for example in the nuclear factor κB (NF-κB) pathway (for a review see *e.g*. Jackson *et al*., 2000; Pickart, 2001; Deshaies and Joazeiro, 2009; Komander, 2009; Metzger *et al*., 2012).

Proteins are ubiquitinated through an enzymatic cascade involving three enzymes – ubiquitin-activating (E1), ubiquitin-conjugating (E2) and ubiquitin-ligating (E3) enzymes (Fig. 2). Ubiquitin is activated in an ATP-dependent process, which results in a thioester linkage of the ubiquitin C-terminal carboxyl group and the active-site cysteine of an E1 (Pickart *et al*., 2001; Dye and Schulman, 2007). Activated ubiquitin is then transferred to the active-site cysteine of an E2. This E2 with bound ubiquitin next interacts with an E3 ubiquitin ligase, where substrate is bound. This brings them in proximity, so the ubiquitin can be transferred from the E2 to a lysine

residue of substrate. Ubiquitinated substrate can then dissociate from the E3 or can acquire additional ubiquitin modification – another single attachments of ubiquitin or assembly of polyubiquitin chain.

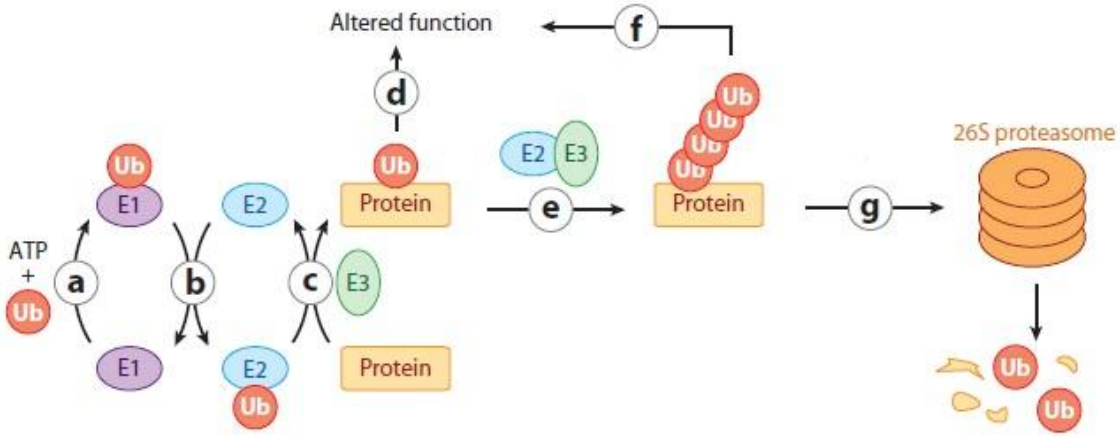

Figure 2: Scheme of the ubiquitin system
Ubiquitin is activated by E1 (a) and transferred to active-site cysteine of an E2 (b). E2-Ub thioester then interacts with an E3, which mediates the transfer of Ub to the substrate (c). Such monoubiquitinated substrate can dissociate from E3 (d) or may require additional Ub attachments (e) to alter its function (f) or to be degraded in 26S proteasome (g) (Deshaies and Joazeiro, 2009; modified).

Ubiquitin can bind via seven different lysine residues (K6, K11, K27, K29, K33, K48, K63). The attachment of ubiquitin via its N-terminal methionine has been also described (Ciechanover and Ben-Saadon, 2004). The linkage type and formation of ubiquitin chains by monoubiquitination, multimonoubiquitination or polyubiquitination determine destiny of proteins. For example, polyubiquitin chain knit via the Lys48 residues of ubiquitin predicts the substrate for proteasomal degradation. In contrast, monoubiquitination or some other types of ubiquitin chains, for example assembled via Lys63, mainly alter the function and localization of modified proteins (Deshaies and Joazeiro, 2009). Ubiquitin labeling is a reversible process, involving deubiquitinases (DUBs) that cleave ubiquitin from its target (Wolberger, 2014).

Substrate specificity is mainly defined by the multiple E2 and E3 combinations possible. Both E2s and E3s belong to large protein families. In mammals, there are about 40 different E2s (van Wijk and Timmers, 2010) and more than 600 putative E3s (Li *et al*., 2008). While E2s share many well-conserved domains, E3s share little sequence homology with the exception of a catalytic domain, what makes them more specific. Based on the type of catalytic domain and the mechanism by which ubiquitin is transferred from the E2 to a substrate, E3 ubiquitin ligases fall into three main classes. The homology to the E6-AP carboxyl terminus (HECT) and the RING-between-RING (RBR) family E3s ubiquitinate substrates in a two-step reaction in which ubiquitin is transferred from the E2 to an active site cysteine in the E3 and then from

the E3 to the substrate (Huibregtse *et al*., 1995; Wenzel and Klevit, 2012). In contrast, the third E3 ubiquitin ligase class, the really interesting new gene (RING) family functions as a scaffold bringing E2s to close proximity of substrates, which facilitates direct transfer of ubiquitin from the E2 enzyme to the substrate (Jackson *et al*., 2000; Deshaies and Joazeiro, 2009; Budhidarmo *et al*., 2012).

2.1.1. RING E3 ligases

The vast majority of E3 enzymes belong to the RING group. A canonical RING domain consists of a series of specifically spaced cysteine and histidine residues, which coordinate two zinc ions (Fig. 3). They together form two loops, each with one zinc ion and central α-helix which serves as conserved platform for E2 binding (Freemont *et al*., 1991).

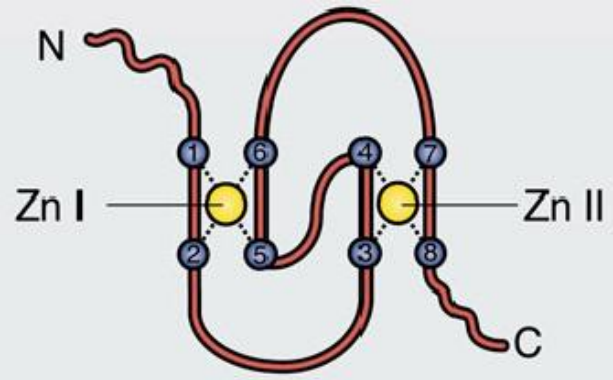

Figure 3: Primary sequence organization of the RING domain
Two zinc ions are coordinated by specifically spaced cysteine and histidine residues (Metzger *et al.*, 2014; modified).

RING E3 ligases can exist as monomers or they can function as dimers or multi-subunit complexes, while dimerization generally occurs through their RING domain or surrounding regions. Dimerization can result in homodimers, *e.g.* cIAP – cellular inhibitor of apoptosis (Mace *et al*., 2008), or heterodimers (*e.g*. MDM2 – murine double minute 2 and MDMX; BRCA1 – breast cancer 1 and BARD1 – BRCA1-associated RING domain 1) (Sharp *et al*., 1999; Brzovic e*t al*., 2001; Linke *et al*., 2008). In both types of dimerization, the two RINGs are in the position that the E2 binding surfaces face away from each other, so direct interaction of the two E2s is unlikely. Both RING E3s of a homodimeric complex have intrinsic capacity to functionally interact with E2s, but this is not the case for some heterodimeric RINGs. Some of them just serve to enhance activity of the second RING, or they can potentially interact with substrates, or in the case of BRCA-1 – BARD-1, to stabilize the complex. The lack of E2 binding activity

of BARD-1 can be attributed to the absence of a portion of the conserved central α-helix (Brzovic *et al.*, 2001).

Binding to substrate occurs generally through other regions of E3 than the RING domain (reviewed in Metzger *et al.*, 2014). One RING E3 may have multiple substrates and several E3s can have the same substrate. For their interaction, they have to be in the same cellular compartment while some RING E3s have nuclear localization and others are transmembrane proteins targeted to endoplasmic reticulum, plasma membrane, peroxisomes, endosomes or Golgi complex. The enzyme-substrate recognition mechanisms are highly varied and occur within networks of interactions including HECT E3s and DUBs. However, the fact is that substrates for most RING E3:E2 pairs are not yet known.

Generally, RING E3 serves as a molecular scaffold to position E2-Ub relative to substrate, but also it serves as an activator of E2-Ub conjugates. A study of E2-Ub conjugates established their dynamic nature in the mean that they adopt an array of the "open" and "closed" conformations. In the absence of E3, E2-Ub is in open conformation. Binding of E3 promotes a conformational change from open to closed state, which primes the active site of E2 to stimulate Ub transfer (Pruneda *et al.*, 2012).

2.1.2. Cullin RING ligases

Some of the RING E3s exist as multi-subunit complexes. The best example of these complexes is the Cullin RING Ligase (CRL) superfamily, which is known for its enormous plasticity in substrate specificity (reviewed in Petroski and Deshaies, 2005). Cullin RING ligase usually consists of at least four proteins – a Cullin (CUL), an adaptor protein, a substrate receptor and a RING protein. The biggest one is CUL – a protein of oblong shape with typical presence of a globular C-terminal domain – cullin homology domain (CHD) and a series of N-terminal repeats of a five helix bundle. Human cells express 8 different CULs (CUL1, 2, 3, 4A, 4B, 5, 7 and PARC). Also, some other proteins contain CHD, for example APC2 - a subunit of anaphase promoting complex (APC/C). To the N-terminal domain of CUL is bound an adaptor protein, specific for each CUL and it is attached to protein carrying motif for recognition of substrate receptor. Another indispensable unit of CRLs is a RING protein which binds to the C-terminal domain of CUL and serves as a docking site for E2s.

The typical CRL is CRL-1, also named as SCF, which consists of S-phase kinase associated protein 1 (SKP1), CUL1 and F-box protein. In this case, the adaptor protein is represented by SKP1, which links the CUL1 and F-box protein and recruits substrate receptors. The RING subunit known as RBX1, ROC1 or HRT1 binds to C-terminal domain of CUL1,

recruits E2s and together they form the active ligase complex (Fig. 4). SCF substrates are bound by one of ~69 interchangeable F-box proteins in humans, carrying the motif for substrate binding, which can potentially recognize substrates (Cenciarelli *et al.*, 1999; Winston *et al.*, 1999; Jin *et al*., 2004). Phosphorylation of target substrates appears to be required for binding the F-box family proteins. For example, one of the highly studied F-box protein – β-TrCP, recognizes a specific phosphoserine motif found in transcriptional regulators β-catenin and IκB – a negative regulator of NF-κB signaling (Winston *et al*., 1999).

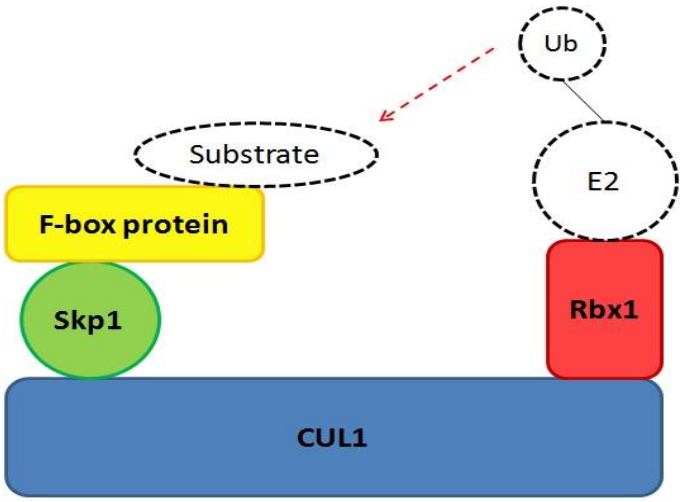

Figure 4: The schematic representation of SCF ubiquitin ligase complex
The catalytic core consists of RING protein – RBX1, which binds an E2, and CUL1, whereas the substrate specificity confers the F-box protein with motif for substrate receptor, linked to the CUL1 through an adaptor protein SKP1.

Another example of RING E3 multi-subunit complex is the anaphase promoting complex/cyclosome (APC/C) which is responsible for correct progression of the cell cycle. This complex consists of 13 core subunits including Apc2, small RING protein (Apc11) and it also contains two interchangeable co-activator subunits – Cdc20 and Cdh1 which are active during different phases of cell cycle and they can recognize distinct substrates (Schreiber *et al*., 2011).

2.1.3. RING ligases and diseases

Mutations of RING E3s or modulation of their activities in other ways are often associated with a variety of human diseases, particularly with cancer (for a review see *e.g.* Lipkowitz and Weissman, 2011; Zhao and Sun, 2013). As an example can be mentioned BRCA1, an E3 playing a critical role in DNA repair and mutated in familial breast and ovarian cancers (Welcsh and King, 2001). Increased activity of Mdm2 ubiquitin ligase, a negative regulator of tumor suppressor p53, is also associated with cancer (Fakharzadeh *et al*., 1991). Another example

of disease in which RING E3 plays a role can be the multisystemic Fanconi anemia, caused by mutations in components of FANC ubiquitin ligase. This disease is characterized by severe developmental defects and increased risk of tumor development (Moldovan and D´Andrea, 2009).

Finally, the majority of individual CRLs are not a *bona fide* tumor suppressor or oncogene by itself, but many of them have been linked to the regulation of oncogenic factors or tumor suppressors to regulate cancer development. Altogether, RING E3s represent attractive targets for development of new anti-cancer therapies or can serve as cancer biomarkers. Despite intense research efforts, many important pieces of the complex puzzle of ubiquitination remain missing. Undoubtedly, an important trail lies in studying of physiological partners of particular E3 ligases, their biological functions and mechanisms of enzyme-substrate recognition.

2.2. Ring finger protein 121

RING finger protein 121 (RNF121) was first described in *C. elegans* as an endoplasmic reticulum (ER) localized ubiquitin E3 ligase, where is involved in ER stress and regulates distal tip cell migration (Darom *et al*., 2010; Kovacevic *et al*., 2012). RNF121 is a well conserved protein, which points to evolutionary important function for this E3 ligase (Zhao *et al*., 2014). In contrast to *C. elegans*, mammal RNF121 appeared to be anchored in Golgi apparatus (Zemirli *et al*., 2014; Zhao *et al*., 2014), however other authors have described it as an ER resident protein (Ogino e*t al*., 2014, Maghsoudlou *et al.*, 2015).

Human RNF121 is located on chromosome 11q13.4 and comprises nine exons and eight introns. The protein consists of 327 amino acids, but the exact topology is not known yet. Five (Zhao *et al.*, 2014) to six (Darom. *et al*., 2010; Maghsoudlou *et al.*, 2015) conserved transmembrane domains have been predicted and the RING-H2 domain, whose orientation is also described in different ways (Fig. 5). The *Rnf121* mRNA is expressed in a variety of human tissues, including heart, lungs, liver, brain, skeletal muscles, placenta or endothelial cells (Zhao *et al.*, 2014).

RNF121 was described to have several roles. In 2014, Zemirli N. and her colleagues reported that RNF121 is an enhancer of NF-κB signaling pathway and it protects cells from cell death. The activation of this pathway involves inhibition of the inhibitory IκB proteins. By using siRNA against RNF121, the proteosomal degradation of IκBα was hampered and in addition, p65/p50 NF-κB dimer levels in nuclear fractions were reduced. Its ability to activate NF-κB was dependent on catalytic activity of RING domain, because mutations in this area caused significantly lower activity of NF-κB. However, RNF121 did not ubiquitinate IκBα directly, though they were found in the same immuno-complex. Authors then hypothesized that RNF121

could control $SCF^{\beta\text{-}TrCP}$ function on IκBα in a complex through ubiquitination. In addition, they found out that a significant pool of β-TrCP2 co-localized with the Golgi apparatus in the area where RNF121 is anchored. Also, they did not rule out the possibility that RNF121 also ubiquitinate other proteins of the SCF complex including Skp1, Cul1 or Rbx1/Roc1 (Zemirli e*t al*., 2014).

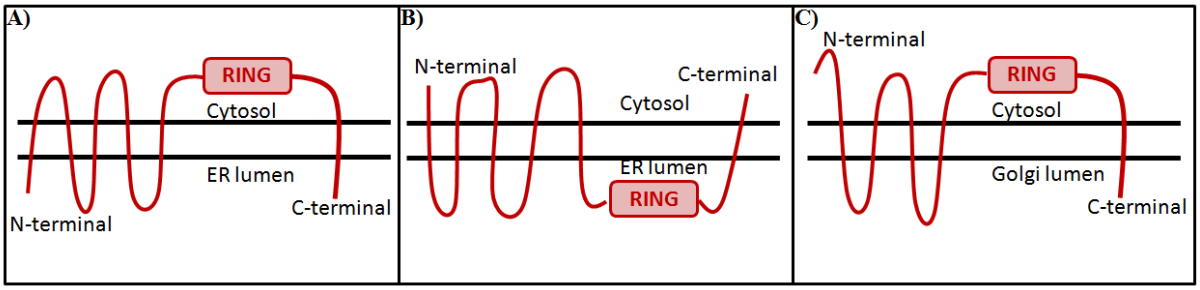

Figure 5: Predicted topologies of RNF121 protein

(A) According to Darom and his colleagues (2010), the RNF121 is an ER-associated protein having 6 transmembrane domains and the RING domain facing cytosol. The topology was predicted by computer algorithms: PSIPRED, Polyphobius, TMpred, SPLIT, SOSUI, TMHMM2.0 and ConSeq. (B) A RNF121 topology prediction described by Maghsoudlou *et al.* (2015) using Phyre prediction program. (C) The topology of RNF121 presented by Zhao *et al*. (2014). Prediction was based on TopPred and TMpred databases.

Supporting previous findings, Zhao Y. and his colleagues reported that RNF121 functions as a negative regulator of apoptosis (Zhao Y. e*t al*., 2014). Knockdown of RNF121 in human cell lines (MCF-7, HeLa, U2OS) inhibited cell growth and induced apoptosis and also increased the cleaving of caspase-3 and its substrate poly (ADP-ribose) polymerase (PARP). These data indicate that silenced expression of RNF121 induced apoptosis at least in part via caspase signaling. Their findings also pointed to RNF121 as a potential target for cancer therapy, because the RNF121 knockdown significantly enhanced apoptosis induced by etoposid (VP-16), an agent commonly used in cancer chemotherapy that promotes cancer cell apoptosis.

Most likely, RNF121 has a role in quality control of membrane proteins, too. Ogino and his colleagues (Ogino *et al.*, 2015) published a study based on zebrafish RNF121 homolog, called *alligator*. Their findings suggested the participation of RNF121 in the quality control of voltage-gated sodium (Na_V) channels via ubiquitination of misfolded Na_V proteins and transporting properly folded proteins to the membrane of excitable cells. Most recently, RNF121 was shown to bind and ubiquitinate newly synthesized immature vascular endothelial growth factor receptor-2 (VEGFR-2; Maghsoudlou *et al.*, 2015). This receptor is present in endothelial cells with a critical role in physiological and pathological (*e.g.* tumorigenesis) angiogenesis. This ubiquitination inhibits its trafficking from endoplasmic reticulum to Golgi apparatus, restricting its expression at the cell surface and thus minimizing the VEGF angiogenic

signaling in endothelial cells. This process causes significantly reduced angiogenesis and proliferation of endothelial cells, which are the most critical processes in tumor growth and metastasis.

Last but not least, RNF121 may be involved also in tumorigenesis as it was shown that *RNF121* mRNA expression was up to 16.4 times higher in esophageal adenocarcinoma and also in its precancerous stage – Barrett esophagus of than in healthy population (Wang *et al.*, 2014). In addition, RNF121 is located on chromosome 11q13, in a candidate region, which may contain breast cancer susceptibility gene(s) (Rosa-Rosa *et al.*, 2009).

Taken together, the precise mechanism of RNF121 function is still not clear. It will be important to find out direct interacting partners or substrates for RNF121.

2.2.1. *Rnf121* knockout mouse model

Mice carrying a deletion in *Rnf121* exon 4 (*Rnf121*$^{tm1b(EUCOMM)Hmgu}$) were prepared by using embryonic stem (ES) cells in the Czech Centre for Phenogenomics (http://www.phenogenomics.cz/). A targeting vector introduced into ES cells was designed in the way that it allows to produce reporter (LacZ) knockout, conditional knockout, and null allele following exposure to site-specific recombinases Cre and Flp (EUCOMM allele, Fig. 6). C57Bl/6N mice harboring a knockout-first allele at the *Rnf121* locus were crossed with a C57Bl/6 Cre deleter mouse to remove the neomycin cassette and generate an *Rnf121* allele with deleted exon 4 that creates a frame-shift mutation.

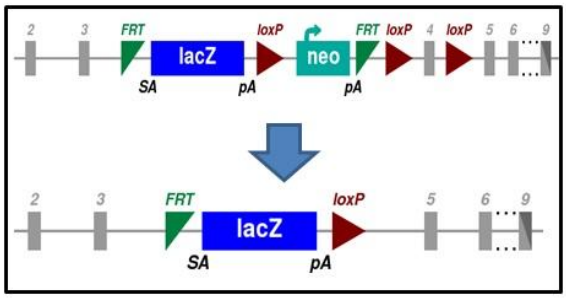

Fig 6: Generation of *Rnf121* knockout mice

Intercross breeding (*Rnf121*$^{+/-}$ x *Rnf121*$^{+/-}$) repeatedly showed that loss of function of *Rnf121* results in a prenatal phenotype and *Rnf121*$^{-/-}$ embryos die prior embryonic day (E) 11.5. Examination of earlier embryonic stages (E9.5-10.5) revealed severe vascular defects in embryo, yolk sac and placenta (Kallayanee Chawengsaksophak Ph.D., IMG; unpublished). While the vascular formation of the yolk sac of *Rnf121*$^{-/-}$ embryos was almost completely reduced,

the vascularization of the placenta seemed also less developed. In addition, *Rnf121*$^{-/-}$ embryos showed multiple signs of hemorrhage and they were smaller than their *Rnf121*$^{+/+}$ littermates (Fig. 7). These findings pointed out that RNF121 might have a role, among others, in the vascular development.

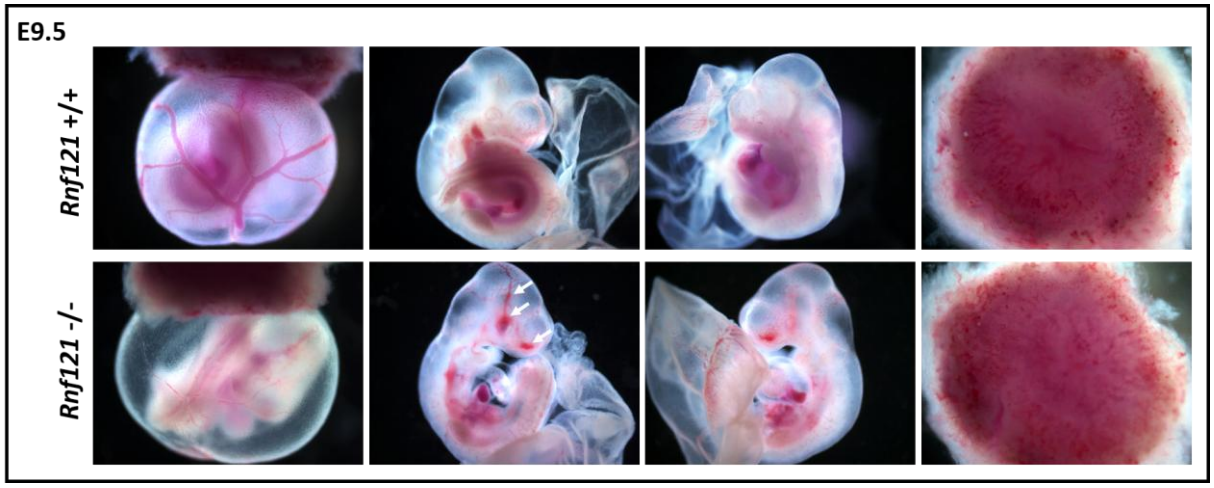

Figure 7: *Rnf121*$^{-/-}$ mouse embryos exhibit severe vascular defects
Comparing the *Rnf121*$^{+/+}$ and *Rnf121*$^{-/-}$ phenotype, numerous vascular defects are apparent in the *Rnf121*$^{-/-}$ embryo and placenta. Arrows points to sites of haemorrhage (Kallayanee Chawengsaksophak, IMG; unpublished.)

2.3. Vascular development

The cardiovascular system is the first organ system, which becomes functional in the developing mouse embryo and its proper functioning is critical for the homeostasis and continued embryonic growth. Two fundamental mechanisms are essential for the blood vessel formation, vasculogenesis and angiogenesis. The vasculogenesis is *de novo* formation of endothelial cells from mesenchymal precursors – angioblasts (His, 1900). In contrast, the angiogenesis is a process generating new blood vessels by sprouting from preexisting ones and it is driven by endothelial cells proliferation. If both of these processes work well, it leads to the gradual maturation of the vascular system into its final form containing completely developed veins, venules, arteries and arterioles.

The vasculogenesis is then divided as extraembryonic and intraembryonic. The extraembryonic vasculogenesis occurs first, which is initially apparent as blood islands within the mesodermal layer of the yolk sac. Blood islands are composed of inner mass of embryonic hematopoietic precursors and an outer layer of angioblasts. The coalescence of blood islands forms functional vessels, which can communicate with the developing fetus via the vitelline vein, but they do not contribute to the development of intraembryonic vasculature. Another structure

where extraembryonic vasculogenesis also occurs is the allantois, a mesodermal part of the placenta (reviewed in *e.g.* Maltepe and Simon, 1998; Drake, 2003).

2.3.1. Placenta vascular development

The placenta is an organ essential for survival and growth of the fetus during gestation. It forms the interface between the fetal and maternal environment and it performs many critical functions, such as transfer of nutrients, exchange of gases between mother and the fetus, disposal of fetal metabolic products. Placenta has also an endocrine function, because it produces some gestation-related hormones, which alter the physiology of mother during the pregnancy and are essential for fetal developing. In addition, placenta acts as a barrier against the maternal immune system (for a review see *e.g*. Rossant and Cross, 2001; Watson and Cross, 2005).

In rodents, the placental development begins at the blastocyst stage, which corresponds to E3.5 (Fig. 8). The trophectoderm cells, which are not directly attached to the inner cell mass (ICM) of the blastocyst, give rise to primary trophoblast giant cells (TGCs). TGCs are a source of luteotrophic and lactogenic hormones (Soares *et al*., 1998) and also produce angiogenic factors, VEGF (Shweiki *et al*., 1993; Achen *et al*., 1997), proliferin (Jackson e*t al*., 1994), and vasodilatator – adrenomodulin (Yotsumoto *et al*., 1998) which promote maternal blood flow to the site of implantation. Secondary TGCs are derived later in gestation from cell layer called spongiotrophoblast (Cross, 2000). By the time of implantation (E4.5), TGCs stop dividing and undergo the process of endoreduplication and thus become polyploid.

In contrast, polar trophectoderm cells attached to the ICM continue to proliferate and emerge to diploid cells of extraembryonic ectoderm and ectoplacental cone (Copp, 1979). The extraembryonic ectoderm gives rise to trophoblast cells of the chorion layer, which later develop into labyrinth. Another structure of the placenta – allantois, derives from mesoderm at the posterior end of the embryo at E8.0 (Cross e*t al*., 2003), and at around E8.5 participates together with the chorion in the process called chorioallantoic attachment (Downs, 1998). Defects in this process are responsible for most cases of the midgestation embryonic lethality.

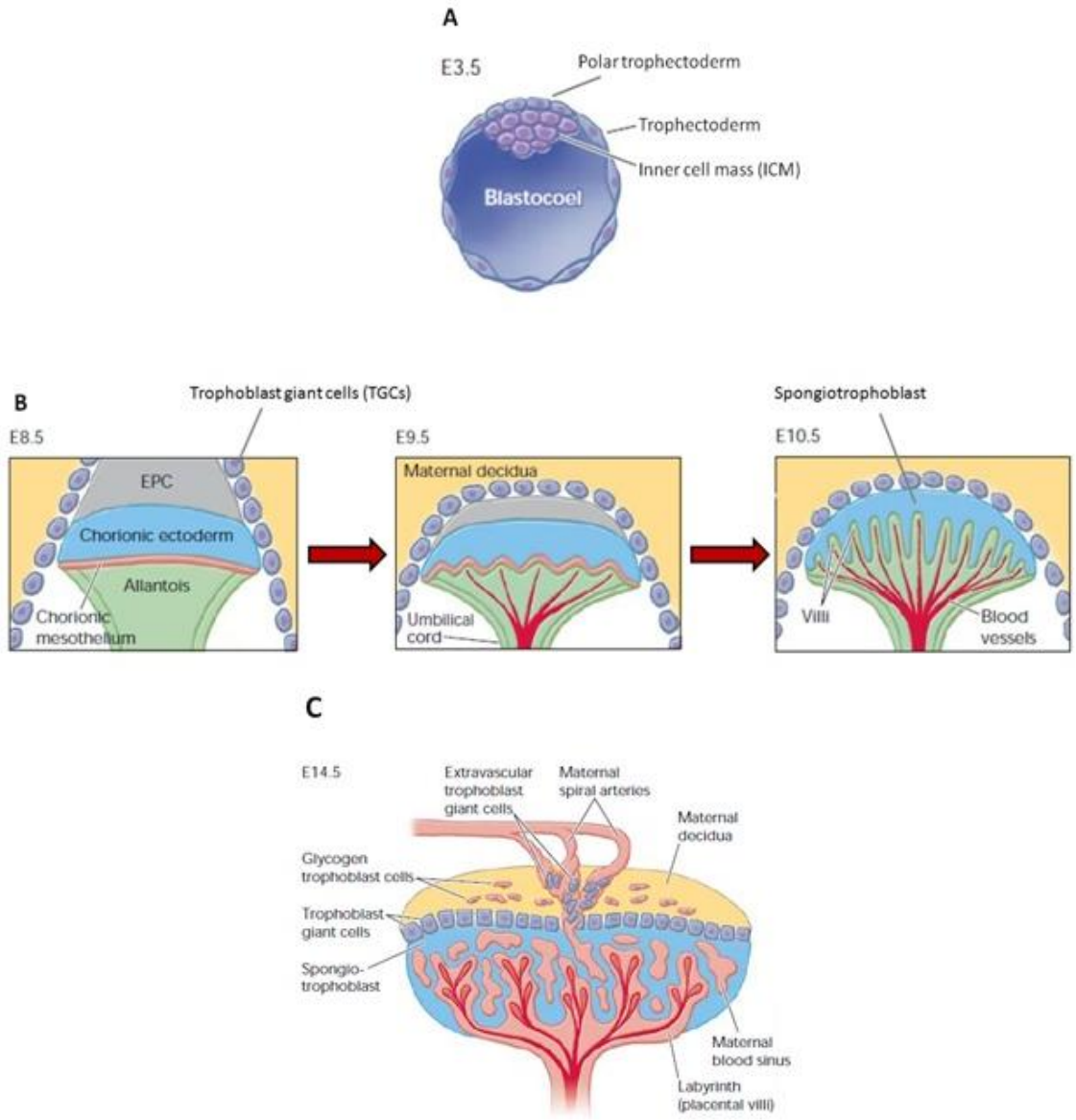

Figure 8: The development of murine placenta

(A) The formation of extraembryonic parts begins at E3.5, at the stage of blastocyst from trophectoderm cells. (B) After the choriollantoic attachment at E8.5, branching morphogenesis in the labyrinth occurs, creating the villi in which the allantois-derived feto-placental blood vessels grow. (C) At E14.5 the placenta can be considered as mature, consisting of three layers: the labyrinth, the spongiotrophoblast and the maternal decidua (Watson and Cross, 2005; modified).

Soon after the chorio-allantoic attachment, folds appear in the chorion, creating the villi and thus defining the space in which the allantois-derived feto-placental blood vessels growth. Meanwhile, the trophoblast cells of the chorion begin to create two types of labyrinth cells. First of them – syncytiotrophoblast, are cells formed by fusion of trophoblast cells and surround the endothelium of the fetal capillaries. The second type is mononuclear and lines the maternal

sinuses. Together, the trophoblast and its associated fetal vasculature form extensively branched villi of the labyrinth. The labyrinth development is structurally supported by spongiotrophoblast, a structure derived from ectoplacental cone, which forms a compact layer between the labyrinth and the trophoblast giant cells (Rossant and Cross, 2001). In later stage of the gestation, the ectoplacental cone gives rise also to the glycogen trophoblast cells, which migrate towards the maternal decidua and at the end of gestation enter into lytic phase and form large lacunae filled with glycogen. These lacunae may provide a substantial source of energy at the end of gestation (Adamson *et al*., 2002; Bouillot *et al*., 2006).

The maternal blood flows through the decidua, the maternal part of the placenta, passes the spongiotrophoblast layer via large sinuses inside and enters into small spaces in the labyrinth, where it bathes the fetal villi and thus allows the exchange of materials between maternal and fetal blood systems. Finally, the umbilical cord, which arose from the allantois, connects the placenta vasculature to the developing embryo. Rodents and primates have a haemochorial type of placenta, which means that the uterine epithelium is eroded, enabling the maternal blood directly bath the trophoblast surface (Wooding and Flint, 2004). The labyrinth development depends on some critical signaling pathways, such as Egf (Threadgill *et al*., 1995), Fgf (Xu *et al*., 1998), Notch (Krebs *et al*., 2000) and Wnt (Monkley *et al*., 1996). If the labyrinth is not developed properly and the placental perfusion is impaired, nutrient and oxygen diffusion is insufficient. In all these cases the lethality is a result of insufficient metabolic exchange.

2.3.2. Intraembryonic vascularization

The development of intraembryonic blood vessels is not dependent on the colonization from the yolk sac as initially expected. The intraembryonic vasculogenesis is iniciated at E7.3 in the cranial region and its active period lasts till E7.8. The first endothelial structures developed in the embryo are the endocardial tube and great vessels (Drake and Fleming, 2000). Also, the initial vascularization of some organs in mice occurs by vasculogenesis rather than angiogenesis. The vasculogenic blood vessel formation was described in the development of the kidney (Robert *et al*., 1998), liver (Matsumoto e*t al*., 2001), lung (deMello *et al*., 1997) and pancreas (Lammert *et al*., 2001), related to growth of the tissue, providing for the metabolic needs of surrounding cells.

2.3.3. Regulation of vascularization

A number of various proteins, including transcription factors, angiogenic growth factors, cell adhesion molecules and their receptors participate in endothelial differentiation and vessel formation.

2.3.3.1. Vascular endothelial growth factor

Vascular endothelial growth factor (VEGF) and its receptors VEGFR1/Flt1, VEGFR-2/Flk1 were identified as key regulators of vasculogenesis (Drake and Little, 1995). In mammals, there are 5 members of VEGF protein family and the best studied is VEGF-A, called also just VEGF. Alternative splicing of VEGF transcript generates several isoforms which can differ

in their functions. A regulation of embryonic vessel formation by this signal protein is strictly dose-dependent. Embryos lacking a single copy of the VEGF gene exhibit early embryonic lethality, around E10.0, due to impaired intra- and extraembryonic vessel formation and cardiac development. Also blood island formation is impaired. This phenotype is even more appreciable in the homozygotes (Carmeliet *et al*., 1996; Ferrara *et al*., 1996; Risau, 1997).

Cells responding to VEGF signaling must first express VEGF receptors, Flk1 and Flt1. The Flk1 is an important tyrosine kinase receptor regulating distinct cellular processes ranging from developmental vasculogenesis to pathological angiogenesis in tumors (Ferrara, 2004). It is the earliest VEGF receptor expressed, detectable at E7.0, which corresponds to its requirement for endothelial cells precursors development (Dumont *et al.*, 1995). Embryos lacking Flk1 exhibit most severe phenotype. Thus mutant embryos suffer from complete failure of vasculogenesis, endothelial cell differentiation and haematopoiesis (Shalaby e*t al*., 1995). In addition, in yolk sacs of these animals no blood islands can be detected as well as haematopoietic progenitor cells are almost not present (Shalaby e*t al*., 1997). Deficiency of Flt1 leads to less severe phenotype, characterized mainly by enlarged vessels and their disorganized formation.

Before formation of the vasculature, the embryo is situated in a hypoxic atmosphere. This environment activates the hypoxia-inducible factor 1 (HIF-1), a transcription factor which is upstream of VEGF and Flk1 and regulates their expression. It has a crucial role in sensing changes in tissue oxygen tension and stimulating expression of genes which enhances blood vessel growth into hypoxic tissues during embryonic development and tumor formation (reviewed in Ryan and Johnson, 1998; Semenza, 2003; Weidemann and Johnson, 2008). The hypoxic environment of early gestation, and thus the activating of HIF-1, plays an important role in placenta development. The ability of cytotrophoblast cells to invade the uterine vessels

in hypoxic nature of the placenta is dependent on oxygen tension. The cytotrophoblast cells proliferate and continue to move through the placenta until they invade uterine arteries. Then, due to higher concentration of oxygen in arterial blood, they stop dividing and differentiate establishing the uteroplacental circulation (Maltepe and Simon, 1998).

2.3.3.2. Another important factors involved in vascular development

A factor that plays an important role in vascular development is platelet-derived growth factor β (PDGFβ) which serves as structural support for growing vessels in a way, that it recruits pericytes and smooth muscle cells to the endothelial cells and thus establish vasomotor tone (Peppel *et al*., 2005). PDGFβ deficient embryos have vessels without proper pericytes and at late gestation they die due to hemorrhage (Lindahl *et al*., 1997).

Another endothelial specific marker is vascular endothelial (VE) cadherin. It is an adhesive cell-cell recognition protein and in vascular morphogenesis, it participates in cell sorting. VE-cadherin also offers junctional strength between developing endothelial cells due to its ability to anchor to the cortical actin cytoskeleton via catenins and vinculin (Carmeliet *et al*., 1999). VE-cadherin is coexpressed with Flk1 in developing blood vessels, so these receptors should interact (Breier *et al*., 1996).

An important growth factor for cardiac development is angiopoietin-1 (Ang-1) which is a specific ligand for receptor tyrosine kinase Tie-2. Ang-1 is expressed mainly by the mesenchymal cells, which surround developing vessels and in the myocardial layer of the heart. Besides the cardiac development it is also critical in vascular network formation. Mouse embryos deficient for Ang-1 and Tie-2 exhibit normal vasculogenesis, but abnormal heart trabeculae formation together with much less complex vascular network then wild-type littermates (Breier, 2000). Angiopoietin-2, a related factor, has been shown to antagonize with Ang-1 on Tie-2 receptor, so its expression may contribute to blood vessel regression (Maisonpierre *et al*., 1997).

2.4.NF-κB pathway

The ability to respond to external changes is essential for multicellular organisms for surviving, but also for normal development and physiology. Inducible regulation of gene expression allows them adaptation to environmental, chemical, microbiological or mechanical changes. The key roles in these processes have inducible transcription factors such as nuclear factor kappa enhancer binding protein (NF-κB). NF-κB has become the focus of intense research

since it was discovered 30 years ago (Sen and Baltimore, 1986). NF-κB has the most important role in immune system, but also acts to influence gene expression events that have effects on cell survival, proliferation and differentiation. The dysregulation of NF-κB usually leads to severe consequences, including numerous diseases. Its aberrant activation is associated with autoimmune diseases, cancer, cardiovascular diseases, neurodegenerative diseases or diabetes (for a review see *e.g*. Skaug *et al*., 2009; Ben-Neriah and Karin, 2011; Hayden and Ghosh, 2012).

The NF-κB transcription factor family consists of five members in mammals – p50, p52, p65, c-REL and REL-B (Hayden and Ghosh, 2008). p50 and p52 must be produced by proteasomal processing of the p105 and p100 precursors, respectively. All of the members form homo- or heterodimers that occur through an N-terminal REL-homology domain (RHD). RHD is also responsible for interaction with inhibitor of NF-κB (IκB) proteins, nuclear translocation and DNA binding. Under basal conditions, NF-κB dimers are held in inactive state in the cytoplasm through association with IκB proteins. Stimulation of cells with some agonist leads to rapid phosphorylation, ubiquitination and proteasomal degradation of IκBs. The nuclear localization signal (NLS) of p65 is then unmasked and released NF-κB dimers can translocate to the nucleus and regulate transcription of target genes. IκB proteins contain multiple ankyrin repeat domain which binds NF-κB dimers. Also p105 and p100 contain this domain, but it is degraded during processing to p50 and p52, respectively. There are two pathways leading to NF-κB activation – canonical and noncanonical (Fig. 9) (Skaug e*t al*., 2009; Hayden and Ghosh, 2012).

In the case of canonical pathway, cells are stimulated with agonists such as tumor necrosis factor α (TNFα), interleukin-1β (IL-1β) or ligands for Toll-like receptor (TLR). This stimulation leads to activation of transforming growth factor-β-activated kinase (TAK1) complex through TNF receptor-associated factor (TRAF) proteins. TAK1 then activates IκB kinase (IKK) complex which consists of two catalytic subunits – IKKα and IKKβ and one regulatory subunit - NF-κB essential modulator (NEMO). The role of this complex is to phosphorylate IκBα on specific serines – 32 and 36 which leads to recognition by βTrCP proteins of SCF ubiquitin ligase complex. IκBα is then polyubiquitinated on lysines 21 and 22 and degraded by the 26S proteasome (Chen, 2005). Finally, NF-κB dimers accumulate in the nucleus and bind to DNA κB sites and regulate the transcription of target genes.

The noncanonical NF-κB pathway is induced by specific members of TNF receptor superfamily, including those for CD40 ligand, lymphotoxin-β or B-cell activating factor (BAFF) receptor. The noncanonical pathway depends on NF-κB inducing kinase, the IKKα subunit and is independent of NEMO (Senftleben *et al*., 2001; Xiao *et al*., 2001). IKKα phosphorylates p100, which targets it for polyubiquitination and subsequent proteasomal processing to p52.

The p52/REL-B dimer then translocates into the nucleus where it activates gene transcription. In both cases, the transcriptional response is terminated by not only resynthesis of IκB proteins but also by removal of active NF-κB dimers from the DNA.

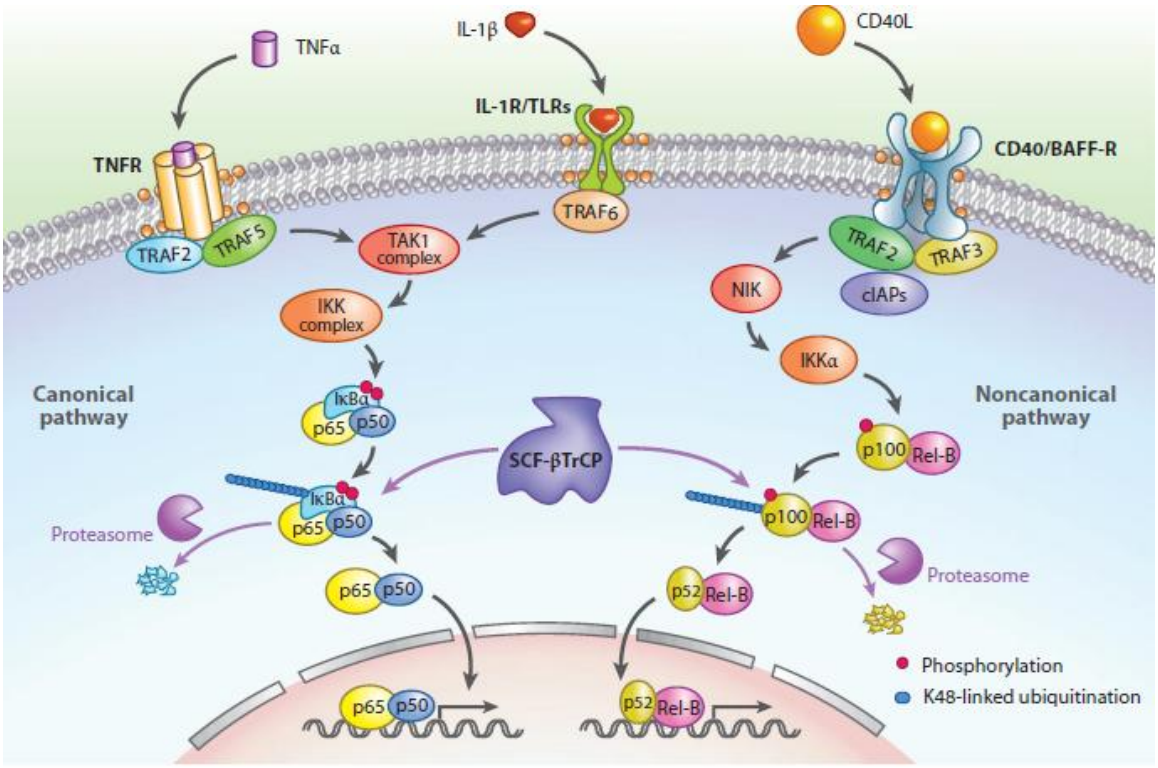

Figure 9: The schematic picture of two pathways leading to NF-κB activation
The canonical pathway: The stimulation of TNF receptor (TNFR), Toll-like receptor (TLR) or IL-1 receptor leads to activation of the TAK1 complex with contribution of TRAF proteins. TAK1 subsequently activates the IKK complex, which phosphorylates the IκBα and by this way targets it for the polyubiquitination by $SCF^{\beta TrCP}$ E3 ligase complex. IκBα is then degraded in the proteasome and p65/p50 NF-κB dimer can enter the nucleus where it triggers the gene transcription.
The non-canonical pathway: The signaling is initiated by stimulation of CD40 or BAFF receptors. The signal is transduced through the TRAF proteins and NIK kinase to the IKKα, which then phosphorylates p100, leading to its ubiquitination and processing to p52. The p52/Rel-B dimer than translocates into the nucleus and activates gene transcription (taken from Skaug e*t al*., 2009).

3. Materials and methods

3.1.Materials

3.1.1. Instruments

-80°C freezer	Sanyo, Japan
Apotome 2.Microscope	Zeiss, Germany
Bioruptor Plus	Diagenode, Belgium
Centrifuge 5424R	Eppendorf, Germany
Centrifuge 5810R	Eppendorf, Germany
Confocal Microscope Leica SP5	Leica Microsystems, Germany
Electrophoresis power supply PowerPac HC	BioRad, USA
Flowbox Bio 2 Advance	Telstar, Spain
Hybridization oven Dry Line Prime	VWR, USA
Imaging system ChemiDoc MP	BioRad, USA
Microscope Axio Imager Z2	Zeiss, Germany
Minicentrifuge FVL 2400N Combi-Spin	BioSan, Latvia
MiniTrans Blot Apparature	BioRad, USA
SDS-PAGE Electrophoresis Apparature	BioRad, USA
Shaker incubator (37°C) Innova 42	New Bruswick Scientific, USA
Spectrofotometr EnVision MultiLabel Reader	PerkinElmer, USA
T100 Thermal cycler	BioRad, USA
Thermoblock Mixing block MB-102	BioER, China
Vortex V-1 Plus	BioSan, Latvia

3.1.2. Bacterial strains and cell lines

DHB10 bacteria: F^- endA1 $deoR^+$ recA1 galE15 galK16 nupG rpsL Δ(lac)X74 φ80lacZΔM15 araD139 Δ(ara,leu)7697 mcrA Δ(mrr-hsdRMS-mcrBC) Str^R λ^-; Invitrogen, USA

XL1 Blue bacteria: endA1 gyrA96(nal^R) thi-1 recA1 relA1 lac glnV44 F'[::Tn10 $proAB^+$ $lacI^q$ Δ(lacZ)M15] hsdR17(r_K^- m_K^+); Stratagene, USA

3.1.3. Chemicals

1xPBS	IMG media facility, Czech Republic
5x Phusion HF Reaction Buffer	New England BioLabs, USA
5x Transcription buffer	Fermentas, Canada
Acetic anhydride	Sigma-Aldrich, USA
Acetyc anhydride	Sigma-Aldrich, USA
Agarose beads - anti-FLAG® M2 Magnetic Beads	Sigma-Aldrich, USA
Ampicillin	Sigma Aldrich, USA
Aquatex mounting medium	Merck Millipore, Germany
Blocking reagent	Roche, Switzerland
BM-purple	Roche, Switzerland
BSA	Carl Roth, Germany
Buffer + $MgCl_2$	Invitrogen, USA
Calcium chloride	Sigma-Aldrich, USA
CHAPS	Sigma-Aldrich, USA
Cumaric Acid	Sigma-Aldrich, USA
DAPI	Sigma-Aldrich, USA
DIG RNA labeling mix	Roche, Switzerland
DNaseI	Invitrogen, USA
dNTP mix (10mM each)	Invitrogen, USA
DreamTaq DNA polymerase	Thermo Fisher Scientific, USA
DreamTaq green buffer 10x	Thermo Fisher Scientific, USA
Dubbelco´s Modified Eagles Medium	Sigma-Aldrich, USA
EDTA	Sigma-Aldrich, USA
Ethanol	Penta, Czech Republic
Fetal bovine serum	Sigma-Aldrich, USA
Fluorescent mounting medium	DAKO, Denmark
Formamide	Sigma-Aldrich, USA
Glucose	Sigma-Aldrich, USA
Glycerol	Lachner, Czech Republic
Glycine	Sigma-Aldrich, USA
H_2O_2	Sigma-Aldrich, USA
Isopropanol	Lachner, Czech Republic

Kanamycin	Sigma Aldrich, USA
LB medium	IMG media facility, Czech Republic
Levamisole	Sigma-Aldrich, USA
Lipofectamine LTX	Sigma-Aldrich, USA
Luminol	Sigma-Aldrich, USA
Maleic acid	Sigma-Aldrich, USA
Manganese chloride	Sigma-Aldrich, USA
Methanol	Penta, Czech Republic
Powder milk	Carl Roth, Germany
MOPS	Carl Roth, Germany
Paraformaldehyde	Sigma-Aldrich, USA
Penicillin-Streptamycin	Sigma-Aldrich, USA
Phusion High Fidelity DNA polymerase	NewEngland Biolabs, USA
Potassium acetate	Sigma-Aldrich, USA
Potassium chloride	Sigma-Aldrich, USA
Proteinase K	Sigma-Aldrich, USA
Quick extract solution	Epicentre, USA
RNase A	Roche, Switzerland
rRNAsin	Promega, USA
SDS	Sigma-Aldrich, USA
Sheep serum	Sigma-Aldrich, USA
SP6 RNA polymerase	Invitrogen, USA
T4 ligase	New England Biolabs, USA
T4 ligase buffer	New England Biolabs, USA
T7 RNA polymerase	Invitrogen, USA
Triethanolamine	Sigma-Aldrich, USA
Triton X-100	Sigma-Aldrich, USA
Trypsin-EDTA solution	Sigma-Aldrich, USA
Tween 20	Sigma-Aldrich, USA
Xylene	Lachner, Czech Republic

3.1.4. Primary Antibodies

Anti-Digoxigenin-AP antibody	Roche, Switzerland
Monoclonal Anti-Flag antibody	Sigma-Aldrich, USA
Polyclonal NF-κB p65 NLS antibody	Novus Biologicals, USA

3.1.5. Secondary antibodies

Alexa Fluor 488 anti-rabbit antibody	ThermoFisher Scientific, USA
Anti-mouse-HRP conjugated antibody	Sigma-Aldrich, USA

3.1.6. Solutions

10x TBS – 250 mM Tris-HCl, pH 7.5, 1.5 M NaCl

10x TBS-T – 250 mM Tris-HCl, pH 7.5, 1.5 M NaCl, 0.5% Tween 20

1x SDS-PAGE sample buffer – 62.5 mM Tris-HCl, pH 6.8, 2% SDS, 10% (v/v) glycerol, 0.002% bromphenol blue, 50 mM 2-mercaptoethanol

1x TAE – 40 mM Tris-base, 20 mM acetic acid, 1 mM EDTA

Acetylation solution (100 ml) – 98 ml H_2O, 1.3 ml triethanolamine, 0.175 ml HCl, 0.25 ml acetic anhydride

Destain solution (200 ml) – 20 ml acetic acid, 100 ml methanol, 80 ml ddH_2O

DMEM culture medium – 10% FBS, 1% Pen/Strep

Hybridization solution (50 ml) - 25 ml Formamide, 12.5 ml 20x SSC, 1g blocking reagent, 0.5 ml 10% Triton X-100, 0.25 g CHAPS, 0.05 g tRNA, 1.25 ml 0.2M EDTA, 0.05 ml heparine 50 mg/ml, ddH_2O to 50 ml

Lysis solution – 0.2 M NaOH, 1% SDS

MAB Solution – 0.5 M maleic acid, 0.75 M NaCl, in ddH_2O, pH 7.5

MAB/Block Solution – 2% Blocking reagent in MAB solution

Neutralyzing solution (100 ml) – 3 M KOAc, pH 6.0, 60 ml 5 M CH_3CO_2K, 11.5 ml CH_3COOH, ddH_2O to 100 ml

Non-denaturing lysis buffer – 20 mM Tris-HCl, pH 8.0, 137 mM NaCl, 1% Triton X-100, 2 mM EDTA, 2 mM sodium pyrophosphae, 25 mM β-glycerophosphate, 1 mM sodium orthovanade, 10% (v/v) glycerol

NT buffer (1 l) - 30 ml 5M NaCl, 50 ml 1M Tris-HCl, pH 7.5, 1 ml 10% Tween 20, ddH_2O to 1 l

NTM buffer (5 ml) – 0.1 ml 5M NaCl, 0.5 ml 1M Tris-HCl, pH 9.5, 0.5 ml 0.5 M $MgCl_2$, 3.9 ml ddH_2O

NTMT Solution (50 ml) – 30 ml ddH_2O, 5 ml 1 M Tris-HCl, pH 9.5, 2.5 ml 1 M $MgCl_2$, 1 ml 5 M NaCl, 0.5 ml 200 mM Levamisole, 0.05 ml Tween 20, ddH_2O to 50 ml

PBT – 0.1% Tween 20 in 1xPBS

Pre-Block solution – 10% sheep serum in MAB/Block solution

Resuspension solution – 50 mM glucose, 10 mM EDTA, 25 mM Tris-HCl, pH 8.0

RNase A Solution – 0.1% RNase A (10 mg/ml) in TNT Solution

Solution I (10 ml) – 5 ml formamide, 2.5 ml 20x SSC, pH 4.5, 1.5 ml ddH_2O, 1 ml 10% SDS

Solution II (10 ml) – 5 ml formamide, 1 ml 20x SSC, pH 4.5, 4 ml ddH_2O, 0.1 ml 10% SDS

TE buffer – 1 mM EDTA, 10 mM Tris-HCl, pH 8.0

TFBI buffer – 30 mM potassium acetate, 50 mM manganese chloride, 100 mM potassium chloride, 10 mM calcium chloride, 15% (v/v) glycerol

TFBII buffer – 10 mM MOPS, pH 7.0, 75 mM calcium chloride, 10 mM potassium chloride, 15% (v/v) glycerol

TNT Solution (50 ml) – 5 ml 5 M NaCl, 0.5 ml 1 M Tris-HCl, pH 7.5, 0.05 ml Tween 20, ddH_2O to 50 ml

Transfer buffer – 25 mM Tris-Base, 192 mM, glycine, 20% methanol

3.1.7. Commercial kits

BCA Protein Assay Kit (ThermoFisher Scientific, USA)

GeneJet Gel Extraction Kit (ThermoFisher Scientific, USA)

GeneJet PCR Purification Kit (ThermoFisher Scientific, USA)

GeneJet Plasmid Miniprep Kit (ThermoFisher Scientific, USA)

3.2. Methods

3.2.1. DNA and RNA cloning techniques

Polymerase chain reaction (PCR)

The PCR reactions used in this work was set up in order to amplify DNA for further cloning, genotyping or for verification of cloning (colony PCR). Composition of these PCR reactions, used primers and thermal profiles are described in Tables 1, 2 and 3:

PCR	Component	Volume (µl)
A	DNA template	0.5
	5x High Fidelity buffer	4
	dNTPs (10 mM)	0.4
	primer forward (10µM)	1
	primer reverse (10µM)	1
	Phusion polymerase (2U/µl)	0.2
	dH_2O	11.9
	Total volume	**20**
B	DNA template	2
	10x Dream Taq buffer	5
	dNTPs (10mM)	2
	primer forward (10µM)	0.5
	primer reverse (10µM)	0.5
	DreamTaq polymerase (5U/µl)	0.2
	dH_2O	39.75
	Total volume	**50**
C	DNA template	2
	10x Dream Taq buffer	2
	dNTPs (10mM)	0.5
	LacZ forward (10µM)	0.5
	tm1bRNF121wt forward (10µM)	0.5
	RNF121 reverse (10µM)	0.75
	DreamTaq polymerase (5U/µl)	0.15
	dH_2O	13.65
	Total volume	**20**
D	DNA template	1
	10x Dream Taq buffer	2
	dNTPs (10mM)	1
	primer forward (10µM)	0.5
	primer reverse (10µM)	0.5
	DreamTaq polymerase (5U/µl)	0.14
	dH_2O	14.85
	Total volume	**20**

Table 1: Components used per individual PCR reactions
A) Amplification of HsRnf121 for cloning into pCMV6-myc-FLAG vector; B) Amplification of Pcdh12/Hbb-bH1 for cloning into pGEM-T easy; C) Genotyping of tm1b *Rnf121* allele; D) Colony PCR using M13 primers.

PCR	Name	Sequence 5´ - 3´
A	hsRNF121_SgfI_fw	ATTGCGATCGCCATGGCGGCAGTGGTGGAG
	hsRNF121_MluI_rev	AATACGCGTTTCCAGGCCCAGGATGTA
B	Pcdh12_fw	CTTTAACCATCCCAGGCAGA
	Pcdh12_rev	CGATGTTAATACGACTCACTATAGGGGATCCAAACACATCCCAACC
	Hbb-bH1_fw	CACTTGCTTTTGCACACTTGA
	Hbb-bH1_rev	TTGTGCTCTCAATGCAGTCC
C	LacZ_fw	ACGGTTTCCATATGGGGATT
	Tm1bwtRnf121_fw	CTTCTGGTTTCCTCATAAGTGC
	Rnf121_rev	GAGTGGGTCTCCAAATCAGC
D	M13_fw	GTAAAACGACGGCCAGT
	M13_rev	AGGAAACAGCTATGACCAT

Table 2: Primers used in this work
A) Amplification of HsRnf121 for cloning into pCMV6-myc-FLAG vector; B) Amplification of Pcdh12/Hbb-bH1 for cloning into pGEM-T easy, underlined sequence corresponds to T7 promoter; C) Genotyping of tm1b *Rnf121* allele; D) Colony PCR using M13 primers.

PCR	Temperature	Duration	PCR	Temperature	Duration
A	98°C	2 min	**B**	95°C	5 min
	98°C	10 s (34x)		95°C	30 s (32x)
	65°C	30 s (34x)		55/54°C	30 s (32x)
	72°C	1 min (34x)		72°C	1 min (32x)
	72°C	5 min		72°C	5 min
C	95°C	5 min	**D**	95°C	5 min
	95°C	30 s (34x)		95°C	30 s (32x)
	62°C	40 s (34x)		62°C	30 s (32x)
	72°C	1 min (34x)		72°C	1 min (32x)
	72°C	5 min		72°C	5 min

Table 3: The thermal profile of PCR reactions
A) Amplification of HsRnf121 for cloning into pCMV6-myc-FLAG vector; B) Amplification of Pcdh12/Hbb-bH1 for cloning into pGEM-T easy; C) Genotyping of tm1b *Rnf121* allele; D) Colony PCR using M13 primers.

Preparation of competent cells by rubidium chloride method

XL1 Blue bacteria from the glycerol stock were inoculated into 400 µl of LB media and shaked at 37°C for 1 h, then 200 µl of this mixture was plated onto agar Petri dish without antibiotics. Next day, a single colony was resuspended in 3 ml of LB media and incubated in shaking incubator overnight (37°C, 200 rpm). After approximately of 16 h of incubation,

1 ml of the culture was added into Erlenmayer flask containing 100 ml of LB media and the bacteria were grown until OD_{600} = 0.5 – 0.7. Bacterial suspension was kept on ice for 15 min and then distributed into 50 ml tubes and centrifuged at 5500 rpm 4°C for 7 min. Supernatant was discarded and the cell pellet was resuspended in 20 ml of TFB I buffer. Cells were kept on ice for 5 min and then centrifuged (5500 rpm, 4°C, 7 min). After discarding of the supernatant, the cell pellet was resuspended in 2 ml of TFB II buffer and chilled on ice for 15 min. Competent cells were distributed in 50 µl aliquotes into pre-chilled tubes, placed immediately onto dry ice and stored at -80°C.

Transformation of bacteria

For each transformation reaction, 50 µl aliquot of competent bacterial cells was used. Cells were slowly thawed, then mixed with 0.5 µl (~500 ng) of plasmid DNA or 5 µl of ligation mixture and incubated on ice for another 10 min. The heat shock was performed at 42°C for 1 min followed by 2 min of cooling on ice. To each tube with transformation mixture 400 µl of LB media was added and cells were shaken at 37°C for 1 h. 200 µl of this mixture was then plated on the LB agar plate containing appropriate antibiotic and plates were incubated at 37°C overnight.

Isolation of plasmid DNA

Single colony was picked using sterile tip and resuspended in 3 ml of LB media supplemented with antibiotics at appropriate concentration (100 µg/ml ampicillin or 50 µg/ml kanamycin). Tubes were then incubated in shaking incubator overnight (37°C, 200 rpm).

Plasmid DNA from grown bacteria was isolated either by alkaline lysis method or by using a plasmid isolation kit. If alkaline lysis method was used, 2 ml of bacterial culture were centrifuged at 15 000 rpm for 1 min. Supernatant was discarded and 100 µl of Resuspension solution was added. Subsequently, samples were vortexed to completely resuspend the cell pellet. 100 µl of Lysis solution was added and the tubes were mixed gently by inverting 5-6 times. Finally, 150 µl of Neutralizing solution was added and tubes were inverted several times in order to precipitate the chromosomal DNA. Tubes were centrifuged at 15 000 rpm for 5 min and the supernatant was transferred to new tubes and the centrifugation was repeated. The supernatant was mixed with 1 volume of chilled isopropanol and 1/10 volume of 3M sodium acetate and mixed by inverting tubes several times. Tubes were incubated at -20°C for 1 h in order to increase the DNA yield. The plasmid DNA precipitate was spinned down (15 000 rpm, 10 min,

4°C). The supernatant was discarded and pellets were washed with chilled 70% (v/v) ethanol (15 000 rpm, 10 min, 4°C). The DNA pellets were air dried, resuspended in 50 µl of TE buffer + RNase (1 mg/ml) or in dH_2O and incubated at 37°C for 20 min. Thus prepared DNA was stored at -20°C.

In case of isolation of plasmid DNA by GeneJET Plasmid Miniprep Kit (Thermo Fisher Scientific, USA), 2 ml of bacterial culture were centrifuged for 2 min (15 000 rpm, RT). Isolation steps were processed according to GeneJET Plasmid Miniprep Kit protocol (available at www.thermofisher.com). The plasmid DNA was eluted in 30 µl of TE or dH_2O.

Agarose Gel electrophoresis

Agarose powder (Lonza, Czech Republic) was dissolved in 1xTAE buffer (for 1% agarose gel, the final concentration was 0.01 g/ml) and completely melted using microwave oven (2-3 min). After the mixture cooled down, ethidium bromide (EtBr) was added and into a final concentration of 0.5 µg/ml. The mixture was poured into the form and it was allowed to solidify. The prepared gel was placed into electrophoresis tank filled with 1xTAE buffer. The electrophoresis was performed at 90 V for approximately 40 min. The DNA/RNA was visualized using ChemiDoc MP System (BioRad, USA).

Restriction of DNA and ligation

Plasmid DNA was mixed with restriction enzyme (1 µg of DNA/1 U of enzyme), 2 µl of corresponding buffer and dH_2O to a final volume of 20 µl. The mixture was incubating for 2-4 h at temperature suitable for the particular enzyme. If needed, the restricted plasmid was extracted from the agarose gel and then purified using GeneJet Gel Extraction Kit (ThermoFisher Scientific, USA)

50 ng of linearized vector DNA were mixed with DNA insert in amount corresponding to molar ratio 1:3 (vector:insert). The mixture was supplemented with 1 µl of T4 DNA ligase (units), 1 µl of T4 DNA ligase buffer (10x) (New England Biolabs, USA) and dH_2O to a final volume of 10 µl and incubated at 16°C overnight. 5 µl of ligation mixture was used for transformation of competent bacterial cells.

Preparing of RNA probes

In order to amplify a DNA region corresponding to a gene of interest, PCR reaction was performed using primers described in Table 2, and the composition of PCR reaction and PCR

program is described in Table 1B and 3B, respectively. As a template, cDNA obtained from E9.5 wt embryo was used. The PCR product was then purified using PCR purification Kit (GeneJET PCR Purification Kit; ThermoFisher Scientific) and the insert was cloned into pGEM-T Easy Vector (Fig. 10; Promega, USA). This vector is linearized with a single 3´-terminal thymidine (T) overhangs at both ends. These T-overhangs prevent recircularization of the vector and provide a compatible overhang for PCR products with A-overhangs generated by majority of DNA polymerases. Transformed DH10B competent cells were plated onto agar plates containing ampicillin and incubated at 37°C overnight. 6 colonies from each plate were picked, resuspended in LB media and verified by colony PCR. DNA from candidate clones was isolated using GeneJet miniprep kit and sent for sequencing. For obtaining DNA template for *in vitro* transcription, PCR amplification using M13 primers was performed to amplify the desired sequence together with T7 and SP6 promoter.

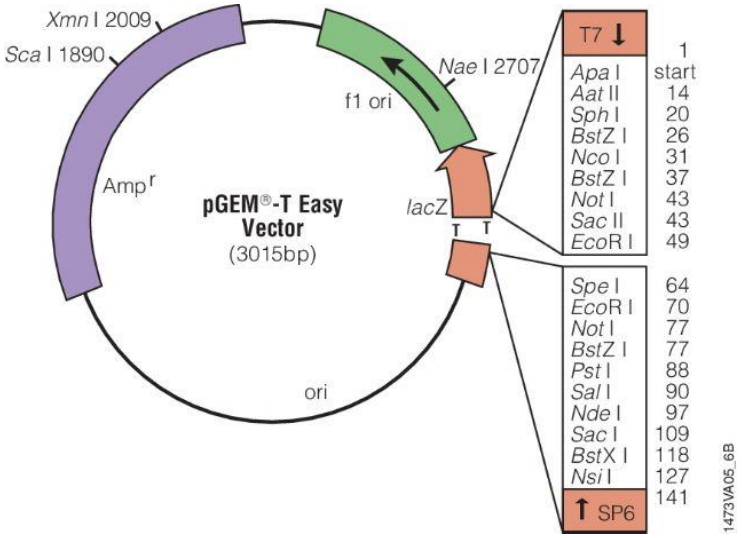

Figure 10: The pGEM-T Easy Vector map (taken from www.promega.com)

PCR products were purified using GeneJet PCR purification Kit (ThermoFisher Scientific, USA) and used as templates for anti-sense and sense Digoxigenin (DIG) labeled RNA probe synthesis. The transcription mixture is described in Table 4. The reaction was performed at 37°C for T7 polymerase and 42°C for SP6 polymerase for 2 h. The *in vitro* transcription products were treated with 1 µl of DNase I (2U/µl). The reaction was supplemented with 2 µl of Buffer+$MgCl_2$ (Thermo Fisher Scientific, USA) and water to a final volume of 20 µl and incubated for 1 h

at 37°C. The resulting RNA was precipitated overnight at -20°C using reagents as described in Table 5. The precipitated RNA was then centrifuged at 14 000 rpm, 4°C, for 30 min, pellets were washed with 75% (v/v) ethanol (14 000 rpm, 4°C, 5 min), dried at RT and resuspended in 50 µl of DEPC H_2O. RNA probes were placed into -80°C for long term storage.

Component	Volume (µl)
DNA (~300-500 ng)	10
5x transcription buffer	3
RNase inhibitor (rRNAsin)	0.5
RNA polymerase (20 U/µl)	0.5
DIG mix	0.5
DEPC water	0.5
Total volume	**15**

Table 4: The composition of one *in vitro* transcription reaction

Component	Volume (µl)
4M LiCl	3.75
0.2M EDTA	3
96% (v/v) ethanol	150

Table 5: Components used for RNA precipitation

Genomic DNA isolation

Tail biopsies were obtained from 3-4 weeks old mice and placed into 1.5 ml tubes. 50 µl of Quick Extract solution (Epicentre, USA) was added into tubes and tails were incubated at 65°C for 20 min. Tubes were then vortexed, each for 20 s and incubated at 98°C for 2 min. Isolated genomic DNA samples were stored at -20°C.

3.2.2. DNA analysis

Genotyping

Genotyping PCR reaction was used in order to detect mice carrying RNF121 tm1b transgene allele. The genomic DNA obtained from tail biopsies was used as a template for PCR reaction. As a positive control was used DNA from heterozygous mouse containing both – a wild

type and transgene allele and as a negative control was used H_2O. The reaction mixture per one PCR reaction, used oligonucleotides and thermal profile of the reaction is described in Table 1, 2 and 3.

Colony PCR

Colony PCR was proceeded in order to verify the correctness of the cloning into pGEM-T easy vector. Colonies from the agar Petri dish were picked with sterile tip and resuspended in LB media. 1 µl of prepared cell suspension was used as a DNA template for control colony PCR using M13 primers (Table 1D, 2D and 3D). The rest of the suspension of candidate clones was inoculated into 3 ml of LB medium supplemented with ampicillin (100 µg/ml) and incubated overnight with shaking at 37°C. Plasmid DNA was isolated using GeneJet Plasmid Miniprep Kit (ThermoFisher Scientific, USA).

3.2.3. Cell culture techniques

Cell culture maintenance

HEK293T cells were cultivated on tissue culture treated plates in DMEM culture medium containing 10% (v/v) fetal bovine serum (FBS) and 1% (v/v) Penicillin/Streptomycin. After reaching of 90% confluency, the medium was discarded and the cells were washed with PBS followed by adding of 0.5 ml of 0.5% (v/v) trypsin/0.53mM EDTA. Cells were then incubated at 37°C for approximately 5 min until the cells detached from the plate. In order to neutralize the trypsin, 4 ml of fresh DMEM medium was added and cells were resuspended in it. 100 µl of this suspension was dropped onto a new tissue culture plate containing 10 ml of DMEM. Cells were incubated at 37°C, 5% CO_2.

Obtaining of mouse embryonic fibroblasts (MEFs)

The belly of killed mouse was washed with 70% (v/v) ethanol and the uterus was cutted out and transferred into sterile 50 ml tube with PBS. Next steps took place in the tissue culture room. The uterus was placed onto Petri dish with sterile PBS and individual embryos were dissected. The E9.5 embryos were placed individually into small dishes and 1 ml of 0.25% (v/v) Trypsin was added. Embryos were cutted into small pieces with sterile scissors and then resuspended using a syringe with needle. The liquid with resuspended MEF cells was transferred

onto 0.1% (w/v) gelatin-coated wells of 12-well plates with 3 ml of MEF DMEM medium. MEF cells were maintained at 37°C, 5% CO_2.

Transfection of cells

HEK293T cells were transfected on 10 cm plate using Lipofectamine LTX (ThermoScientific), after they achieved about 70% of confluence. The transfection mixture was prepared in 2 separate tubes. In one of them, 500 µl of DMEM was mixed with 10 µg of DNA and 5 µl of Plus reagent (diluted 1:3). In the second tube, 500 µl of DMEM was mixed with 12 µl of Lipofectamine LTX. Finally, both mixtures were mixed together, incubated for 5 min at RT and then dropped onto cells washed with PBS. Transfected cells were incubated at 37°C for 2 h and then 10 ml of fresh DMEM was added.

Immunofluorescent staining of the cells

MEF cells were grown on glass coverslips until they reached approximately 70% confluency. The cells were then washed in PBS two times and fixed with 4% (w/v) paraformaldehyde/PBS for 15 min at 37°C. After washing with PBS, cells were permeabilized by incubation in 0.1% (v/v) Triton X-100/PBS (PBT) at RT for 1 min. Cells were then washed with PBS three times and subsequently proceeded to blocking step in 1% (w/v) BSA/PBT overnight at 4°C. Next day, cells were incubated with the primary antibody anti-p65 diluted in 1% (w/v) BSA/PBT (1:100) for 1 h at 4°C. That was followed by washing with PBS three times and incubation with fluorescent anti-rabbit secondary antibody Alexa Fluor 488 diluted in 1% (w/v) BSA/PBT (1:1000) for 1 h in dark at RT. At first, the cells were washed with PBS containing DAPI (1:1000) for 5 min and then with PBS two times. Coverslips with MEF cells were allowed to dry and mounted with 4 µl of Fluorescent mounting medium (Dako, Denmark). Thus prepared samples were visualized by confocal microscope Leica SP5 (Leica Microsystems, Germany) and edited using Fiji software.

Preparation of cell lysates

HEK293T cells cultivated on 10 cm plate were washed with PBS, then treated with 0.5 ml of 0.5% (v/v) Trypsin/0.53mM EDTA (MEFs were treated with 1 ml of 0.25% (v/v) Trypsin) which was stopped by adding of 4 ml PBS in which cells were resuspended. The cells were then collected in 15 ml tube and spinned down on pre-cooled centrifuge (1500 rpm, 4°C, 5 min).

The supernatant was discarded and the pellet was resuspended in 1 ml of fresh PBS and transferred into new 1.5 ml tube. Cells were centrifuged again (15000 rpm, 4°C, 1 min) and the pellet was resuspended in non-denaturing lysis buffer. Thus prepared lysates were sonicated in Bioruptor (Diagenode; 5cycles: 30s ON, 30s OFF at high power) and then centrifuged in pre-cooled centrifuge (15000 rpm, 4°C, 20 min). The supernatant was transferred into a new 1.5 ml tube and stored at -80° C.

3.2.4. Protein techniques

BCA protein assay

BCA Protein Assay Kit (Thermo Fisher Scientific, USA) was used in order to determine the protein concentration in cell lysates. Standard protein samples were prepared according to BCA protein Assay Kit protocol (available on www.thermofisher.com). Protein samples were diluted (1:15) in dH_2O and 25 µl of the sample was pipetted into 96-well plate. 200 µl of working reagent which was prepared by mixing of solution A and B (50:1) was added to the wells with protein samples and standards. The plate was then incubated at 37°C for 30 min. The absorbance was measured at 562 nm by EnVision Multilabel Reader (PerkinElmer, USA). The concentration of the samples was estimated from the BSA standard curve.

Western blotting

Relevant volume of cell lysate representing 30 µg of proteins was mixed with dH_2O and 6x protein loading buffer to a final volume of 18 µl. Samples were incubated at 75°C for 10 min, vortexed and shortly spinned down before loading on the gel.

SDS-PAGE electrophoresis was used for protein separation. The samples were loaded on 10% (v/v) polyacrylamide gel of width of 1 mm and it was run at 120 V for 90 minutes. The 8x6 cm nitrocellulose membrane (0.45 µm pore-size; BioRad, USA) was activated by incubation in dH_2O for 5 min and subsequently in Transfer buffer for 10 min. Blotting sandwich was assembled from the bottom by this way: filter paper, nitrocellulose membrane, polyacrylamide gel, filter paper and placed in the Mini Trans-Blot apparatus (BioRad, USA). Blotting was performed at 60 mA per one membrane for 1 h. The membrane with transferred proteins was then blocked in 5% (w/v) milk in TBS-T for 1 h at RT. Anti-FLAG primary antibody (Sigma-Aldrich, USA) was diluted in 5% (w/v) milk in TBS-T in a ratio 1:2000 and poured onto membrane and incubated overnight at 4°C with shaking. After overnight incubation, the membrane was washed

5 times in TBS-T. Anti-mouse-HRP conjugated secondary antibody (Sigma-Aldrich, USA) was diluted in 5% (w/v) milk in TBS-T (1:10 000) and the membrane was incubated for 1 h. After the washing process in TBS-T, proteins on the membrane were detected by using Luminescent solution (Table 6) which was dropped onto the membrane, covered by plastic foil and the proteins were visualized with ChemiDoc MP System (BioRad, USA).

Component	Volume (µl)
dH_2O	4.16
1.5 M Tris-HCl, pH 8.8	335
Luminol	25
50 mM cumaric acid	25
H_2O_2	4

Table 6: Composition of Luminescent solution

Immunoprecipitation

Lysates used for immunoprecipitation were prepared from a large amount of cells (approximately 9 x 10^7) using non-denaturing buffer. 80 µl of anti-FLAG® M2 Magnetic Beads (50% slurry, ~40 µl of packed beads volume; Sigma-Aldrich,USA) were washed two times with 400 µl of TBS (= 10 packed volumes) and divided into 2 tubes with lysates. Lysates were supplemented with non-denaturing buffer to a final volume of 800 µl and incubated at 4°C overnight with spinning. Next day, tubes were placed on magnetic separator to collect beads and supernatant was removed. The beads were washed three times with 400 µl of TBS. Finally, 20 µl of 1xSDS-PAGE sample buffer was added and agar beads were incubated at 75°C for 10 min. The tubes were placed on magnetic separator and the eluate was collected. At the same time, the Western blotting analysis was performed to check if the protein of interest was eluted. Samples were prepared and loaded on the gel as it is described in Table 7.

The gels run at 120 V for 90 min. After the SDS-PAGE separation of proteins, the 1.5 mm gel was incubated in Coomassie Blue R250 solution overnight at RT with shaking and then destained with Destain solution for 1 h and if needed, repeated two to three times. The 1.0 mm SDS-PAGE was further proceeded for western blotting with anti-FLAG antibody.

	1.5 mm SDS-PAGE (Coomassie staining)			1.0 mm SDS-PAGE (western blotting)		
Sample	**protein lysate**	**6xLD**	**dH_2O**	**protein solution**	**6xLD**	**dH_2O**
Input	30 µg	3 µl	into 18 µl	30 µg	3 µl	into 18 µl
Elution	18 µl	-	-	2 µl	3 µl	13 µl
Supernatant	20 µl	4 µl	-	4 V of Input	3 µl	into 18 µl
Wash1	20 µl	4 µl	-	-	-	-
Wash2	20 µl	4 µl	-	-	-	-
Wash3	20 µl	4 µl	-	-	-	-

Table 7: Composition of samples loaded on SDS-PAGE gels

3.2.5. Histological analysis techniques

Preparing of samples for in situ hybridization

Isolated embryos and placentas were both washed with PBS and fixed overnight in 4% (w/v) PFA at 4°C. That was followed by dehydration process performed by subsequent washing steps in a series of solutions containing increasing concentration of methanol [25% (v/v), 50% (v/v) and 75% (v/v/)] in PBT, each for 5 min and then stored in 100% (v/v/) methanol at -20°C. Placentas were embedded in paraffin blocks, cutted into 4-7 µm thick sections using microtome, mounted onto clean glass slides and air-dried overnight.

Whole mount in situ hybridization

Embryos stored in 100% (v/v) methanol were placed into 4-well plate and rehydrated by washing steps in a series of decreasing concentration of methanol [100% (v/v), 75% (v/v), 50% (v/v), 25% (v/v)] in PBT for 5 min at RT, 210 rpm. To get rid of the methanol completely, embryos were washed twice in PBT for 10 min.

Embryos were digested with proteinase K to remove proteins interacting with the target sequence. The concentration of proteinase K used and the time of incubation depends on the embryonic stage. For embryonic day E9.5, 10 µg/ml of proteinase K was used and embryos were incubated for 5 min. This was followed by agitation in glycine (2 mg/ml) two times for 10 min and washing in PBT for 10 min. Embryos were then post-fixed in 4% (w/v) PFA for 20 min at RT and washed in PBT for 10 min.

Embryos were incubated with pre-warmed hybridization solution at 65°C for 5 h. To prevent the formation of secondary structures of RNA, RNA probes were denatured for 4 min at 80°C and then diluted in pre-warmed hybridization solution to a final concentration

of 500 ng/ml. Hybridization solution in wells was replaced with fresh one containing RNA probes and embryos were incubated overnight at 65°C.

Next day, embryos were washed in a series of solutions: three times in Solution I for 15 min at 55°C and three times in TNT solution for 5 min at RT with shaking. Subsequently, embryos were incubated in RNase A solution for 1 h at 37°C followed by washing in TNT: Solution II (1:1) for 5 min, two times in Solution II for 15 min and finally three times in MAB solution for 5 min, all at RT. Pre-block solution containing 10% sheep serum was added to wells and embryos were incubated for 3 h at RT with gently shaking. Alkaline phosphatase-coupled anti-digoxigenin antibody diluted in 1% sheep serum in Mab/Block solution (1:3000) was added and embryos were incubated overnight at 4°C with shaking. The third day, embryos were washed in MAB Solution, first three times for 10 min and then for 1 h six times. All of those washes were performed at RT at 210 rpm. Finally, the embryos were washed overnight in fresh MAB solution at 4°C.

Embryos were rinsed three times in NTMT solution for 10 min at RT and chromogenic substrate for alkaline phosphatase BM-purple (Roche) was added and embryos were incubated in dark at RT. Embryos were checked approximately every hour until the color was developed. The color reaction was stopped with PBT and embryos were fixed in 4% PFA overnight at 4°C. Embryos were rinsed in PBT and gradually washed in a series of increasing concentration of glycerol [25% (v/v), 50% (v/v), 75% (v/v)] in PBT and finally stored in 100% glycerol at 4°C. Pictures of embryos were taken by Apotome.2 microscope (Zeiss, Germany).

In situ hybridization on paraffin sections

Slides in glass box were placed into the hybridizing oven and pre-heated for 30 min at 65°C to avoid detaching of sections from the slides. Slides were dewaxed in xylene for 10 min for two times and washed in isopropanol:96% ethanol (1:1), 96% ethanol and 70% (v/v) ethanol, in each for 2 min. This was followed by incubation in 0.3% (v/v) H_2O_2 for 20 min, rinsing with dH_2O and incubation in PBS for 5 min.

As in the case of whole mount *in situ* hybridization, the concentration of proteinase K and the time of incubation depends on the embryonic stage. For E9.5 samples, proteinase K at a final concentration of 10 µg/ml was used and incubated during 8 min. Slides were then washed in PBS and sections were fixed with 4% (w/v) PFA for 10 min. Slides were then washed with PBS three times, followed by acetylation step. This step is important for reducing background while inactivating RNases and intensifies the signal of specifically bound RNA probe. Acetylation solution was poured into the box with slides and immediately 250 µl of acetic anhydride was

added directly into the box. Slides were thus incubated for 10 min and then washed in PBS. Slides were placed into the box saturated with a 5xSSC/50% formamide solution to avoid evaporation and pre-hybridized for 4 h in the hybridization oven at 55°C. RNA probes were denatured (4 min, 80°C) and diluted in the hybridization solution to a final concentration of 800 ng/ml. 150 µl of this solution was dropped onto the slides and covered with a parafilm. Hybridization reaction was carried out overnight at 55°C.

After hybridization, slides were washed in 5xSSC, pH 4.5 at 55°C for 10 min, followed by washing in 0.5xSSC, pH 4.5 four times at 55°C for 15 min and once at RT. Slides were washed twice with NT buffer for 10 min at RT and placed into a moist box and sections were blocked with 10% sheep serum/NT buffer for 4 h at RT. The sections were then incubated with anti-DIG antibody diluted in 1% sheep serum/NT buffer (1:2000) overnight at 4°C. Excess antibody was removed by washing in NT buffer three times for 10 min followed by incubating in NTM buffer for 10 min at RT. BM purple was dropped onto the slides and color development was performed in dark at RT. Staining was stopped by PBS and slides were fixed in 4% (w/v) PFA for 20 min at RT. Finally, the samples were mounted with coverslips using Aquatex mounting medium (Merck Millipore). The pictures of slides were taken by Axio Imager Z2 microscope (Zeiss, Germany)

4. Aims of thesis

The main aim of this diploma thesis is to determine the role of murine RNF121 in the embryonic development with focus on placenta forming and vascularization. For this purpose, RNA probes corresponding to genes important in the embryonic and placental development will be prepared and *in situ* hybridization experiments on placenta sections and whole embryos will be performed. Regarding *in vitro* experiments, the first object is to confirm the role of RNF121 as an enhancer of the NF-κB activity on the *Rnf121*$^{-/-}$ mouse model. In an attempt to better understand the role of RNF121 at molecular level, a substrate detection assay will be performed.

5. Results

5.1.*Rnf121* has an important role in the embryonic development

Previous findings carried out in the Laboratory of Transgenic Models of Diseases, Institute of Molecular Genetics of the ASCR, v.v.i., indicated that *Rnf121* gene has an important role in vascular development. Homozygous mutant embryos were found to have numerous vascular defects, including impaired vascularization of the yolk sac and placenta. *Rnf121*$^{-/-}$ embryos were also smaller than their littermates and died at E10.5-11.5. Because the cause(s) of the embryonic death is not known, whether it is a consequence of defects in the embryo itself or in extraembryonic structures or in both, all three structures were inspected in great detail.

Embryos, yolk sacs and placentas at embryonic stages E8.5 to E10.5 were obtained from *Rnf121*$^{+/-}$ mice intercrosses by either Silvia Petrezsélyová, PhD. (IMG) or Kallayanee Chawengsaksophak, PhD. (IMG). A small pieceof yolk sac isolated served as a DNA material for genotyping of individual embryos. An example of genotyping is shown on Figure 11.

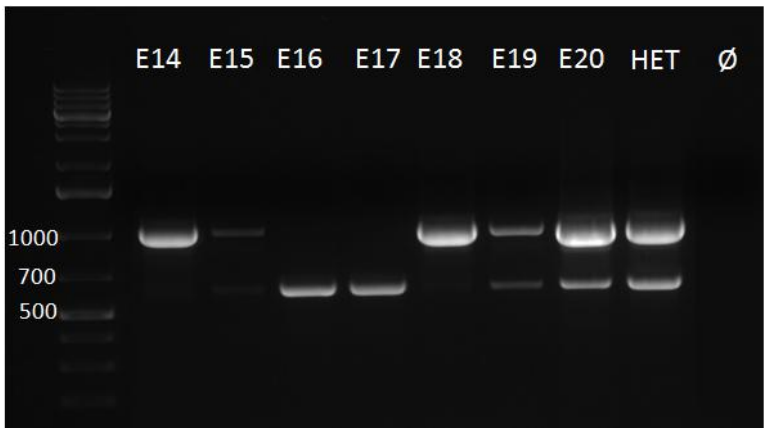

Figure 11: Genotyping of embryos from *Rnf121*$^{+/-}$ intercross
Size of PCR bands: wt allele – 1005 bp, transgene allele – 614 bp. From this intercross, we obtained 2 *Rnf121*$^{+/+}$ (E14 and E18), 3 *Rnf121*$^{+/-}$ (E15, E19 and E20) and 2 *Rnf121*$^{-/-}$ embryos (E16 and E17). HET sample represents a positive control (DNA isolated from tail of an *Rnf121*$^{+/-}$ mouse).PCR reaction with no DNA added served as a negative control (Ø).

5.1.1. *Rnf121* is expressed throughout the embryo

The RNF121 has been demonstrated to be expressed in a variety of adult tissues and cell lines (Zhao *et al*., 2014; Maghsoudlou *et al*., 2015; our laboratory, unpublished). In order to determine the gene expression at embryonic level, mRNA *in situ* hybridization on whole

embryos was performed. The sense and antisense *RNF12* probes were prepared in our laboratory by Christiana Polydorou, PhD.Whole-mount *in situ* hybridization for *RNF121* mRNAshows that is expressed ubiquitously. In the case of embryo hybridized with sense *RNF121* RNA probe, no positive signal was detected, indicating the specificity of anti-sense RNF121 probe binding. To this end, only E9.5 embryos were inspected.

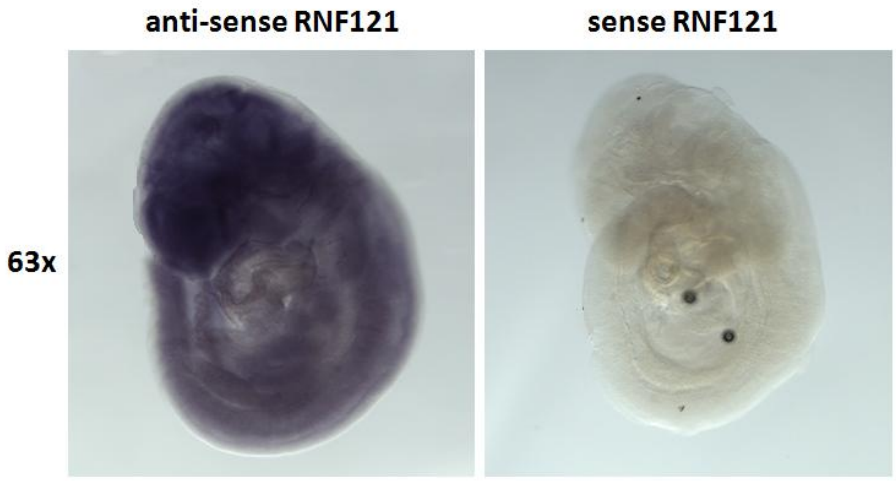

Figure 12: The expression pattern of *RNF121* at E9.5
Wt embryos were hybridized with anti-sense or sense RNF121 probe. At E9.5, the *RNF121* is expressed in whole embryo. The negative control with sense RNA probe showed no signal.

5.1.2. Generation of RNA probes for cell-type specific markers in trophoblast region and yolk sac

One possibility that embryo development is compromised is due to poor placenta formation and function. To analyze the placenta phenotype found in *Rnf121* nulls in more detail, several different trophoblast-specific (*Pl1*, *Hand1* and *Pcdh12*) and fetal endothelial-specific (*Mest*) markers were chosen. To examine the state of primitive proerythroblast formation, mRNA expression of *Hbb-bH1* was examined. For these purposes, *Pcdh12* and *Hbb-bH1* RNA probes were prepared within this work, while the others were prepared in our laboratory by Mgr. Barbora Singerová. Detailed description of these probes is in the Table 8.

Name	Description/Function	Reference
Hand1 (Heart and neural crest derivatives transcript 1)	Expressed by TGC precursors. *Hand1* is essential for early trophoblast differentiation, yolk sac vasculogenesis and heart morphogenesis.	Scott e*t al*., 2000; Simmons *et al*., 2008
Hbb-bH1 (Hemoglobin Z)	Expressed by precursors of yolk sac/embryonic red blood cells - proerythroblasts. *Hbb-bH1* is involved in oxygen binding and transport and heme binding.	This work; McGrath *et al.*, 2003
Mest (Mesoderm specific transcript)	Expresssed since chorioallantoic attachment (E8.5) by fetal endothelial cells lining the fetal capillaries (labyrinth). Mest has a role in placental angiogenesis.	Katsanou et al., 2009; Screen e*t al*., 2008
Pcdh12 (Protocadherin 12)	Expressed by glycogen trophoblast cells (GCs) from E7.5. Function of *Pcdh12* is not well known.	This work; Bouillot *et al*., 2006; Hunkapiller *et al*., 2012
Pl1 (Placental lactogen 1)	Expressed by trophoblast giant cells (TGCs) from E4 to E11. *Pl1* has endocrinal effect on maternal organism.	Kröger *et al*., 2011; Takao *et al*., 2012

Table 8: RNA probes used for section and whole mount *in situ* hybridization
Pcdh12 and *Hbb-bH1* RNA probes were prepared as a part of this diploma thesis, others above mentioned were prepared in our laboratory.

RNA probes were prepared by amplification of *Hbb-bH1* and *Pcdh12* genes by PCR and their subsequent cloning into the pGEM-T easy vector (Promega, USA; vector map is available in the chapter Material and methods). The correctness of cloning was first verified by colony PCR and two candidate clones were sent for sequencing analysis. DNA of verified clones was then amplified from the vector by PCR using M13 primers which was followed by *in vitro* transcription. Thus obtained RNA was treated by DNase (Fig. 13) and used for *in situ* hybridization on placenta sections or whole mount *in situ* hybridization on embryos. Primers for amplification of *Pcdh12* were designed in the way that the sequence for the T7 promoter was already present, therefore, this gene did not have to be cloned into the vector.

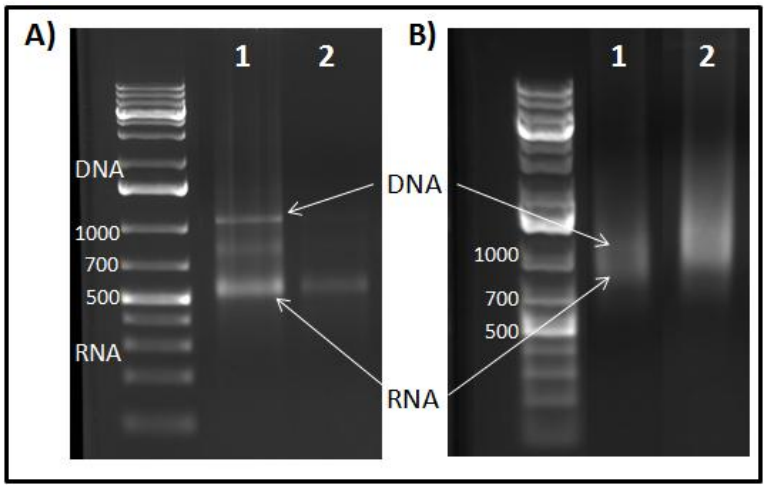

Figure 13: RNA probes after DNase treatment
A) *Pcdh12* – 1: before DNase treatment, 2: after DNase treatment. Into both wells, 1 µl of the reaction was loaded. B) *Hbb-bH1* – 1: before DNase treatment (1 µl of the reaction loaded), 2: after DNase treatment (5 µl of the reaction loaded).

5.1.3. Rnf121$^{-/-}$ embryos suffer from underdeveloped placenta

In order to specify the development of individual placental structures and cell type, the expression of three trophoblast markers (*Hand1, Pl1, Pcdh12*) and one fetal endothelial cell marker (*Mest)* was determined and compared in *Rnf121*$^{+/+}$, *Rnf121*$^{+/-}$ and *Rnf121*$^{-/-}$ littermates. The expression of these genes was also compared in two different embryonic stages – E9.5 and E10.5, which precede the final establishment of the placental phenotype.

Hand1 marker, a gene which is expressed by the TGC precursors, was used for characterization of the trophoblast layer. In overall, this gene is necessary for the early trophoblast differentiation. By E10.5, under physiological conditions, the *Hand1* expression encompasses all three trophoblast layers– labyrinthine, spongiotrophoblast and outer TGC layer (Scott *et al.*, 2000). Our results showed, that *Hand1* was expressed in all *Rnf121*$^{+/+}$, *Rnf121*$^{+/-}$ and *Rnf121*$^{-/-}$ placenta indicating the trophoblast development. However, in the *Rnf121*$^{-/-}$ placenta, the trophoblast layer seemed to be thinner comparing to *Rnf121*$^{+/+}$ and *Rnf121*$^{+/-}$ littermates. The *Hand1* expression was detected in all three trophoblast layers, which is consistent with the publication mentioned above (Fig. 14). It will be necessary to complete these findings with the expression profile of another trophoblast marker *e.g. Mash2*, which acts as an antagonist to *Hand1* and prevents the differentiation of TGCs (Guillemot *et al.*, 1994). By comparing of these two markers, we can get overall characterization of trophoblast development.

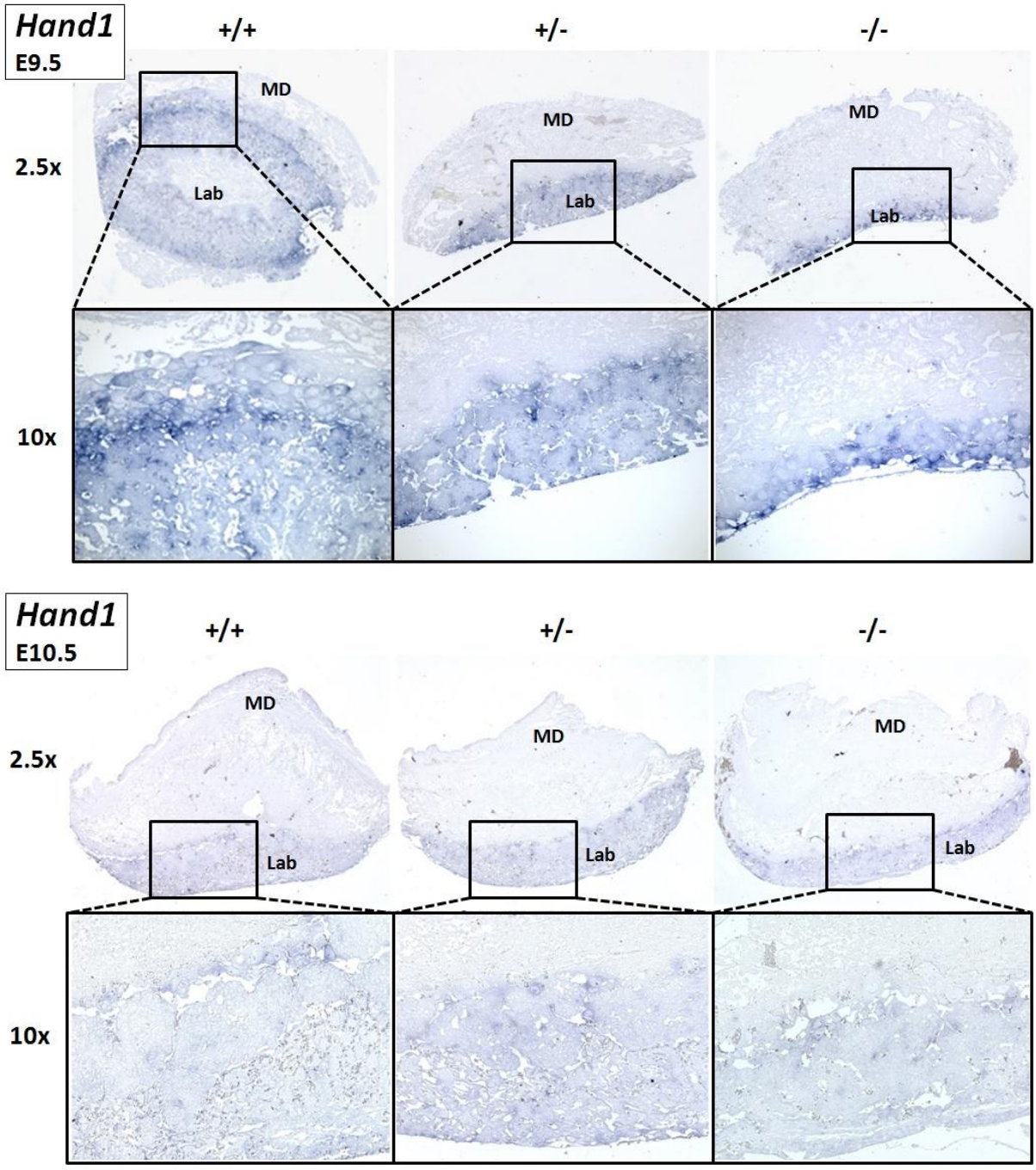

Figure 14: The expression of *Hand1* in *Rnf121* +/+, +/- and -/- placenta
The *Hand1* expression was detected in all three placenta types, tested on both, E9.5 and E10.5 stages. This gene is expressed in all three layers of trophoblast. *Rnf121*$^{-/-}$ placenta shows thinner trophoblast layer. The magnification was 2.5x and 10x, respectively. Lab = Labyrinth, MD = Maternal decidua.

For detection of another cell type within the fetal layer, the *Pl1* marker was chosen. *Pl1* is expressed by TGCs from E4.0 and around E11.0 its expression is disappearing under physiological conditions due to developing another layer of the trophoblast – the spongiotrophoblast (Takeda *et al.*, 2006; Kröger *et al*., 2011). Here it is shown (Fig. 15) that in the case of *Rnf121*$^{+/+}$ placenta, the TGC layer was found out to be receding and far less compact

by the E10.5, compared to E9.5, with gaps in between the individual clusters of cells, indicating the decline of this layer while developing of the spongiotrophoblast. Similar but not the same results were obtained in *Rnf121*$^{+/-}$ placenta. In contrast, in *Rnf121*$^{-/-}$ placenta, the TGC layer was at E10.5 more compact and thicker and the rest of trophoblast layer seemed to be smaller.

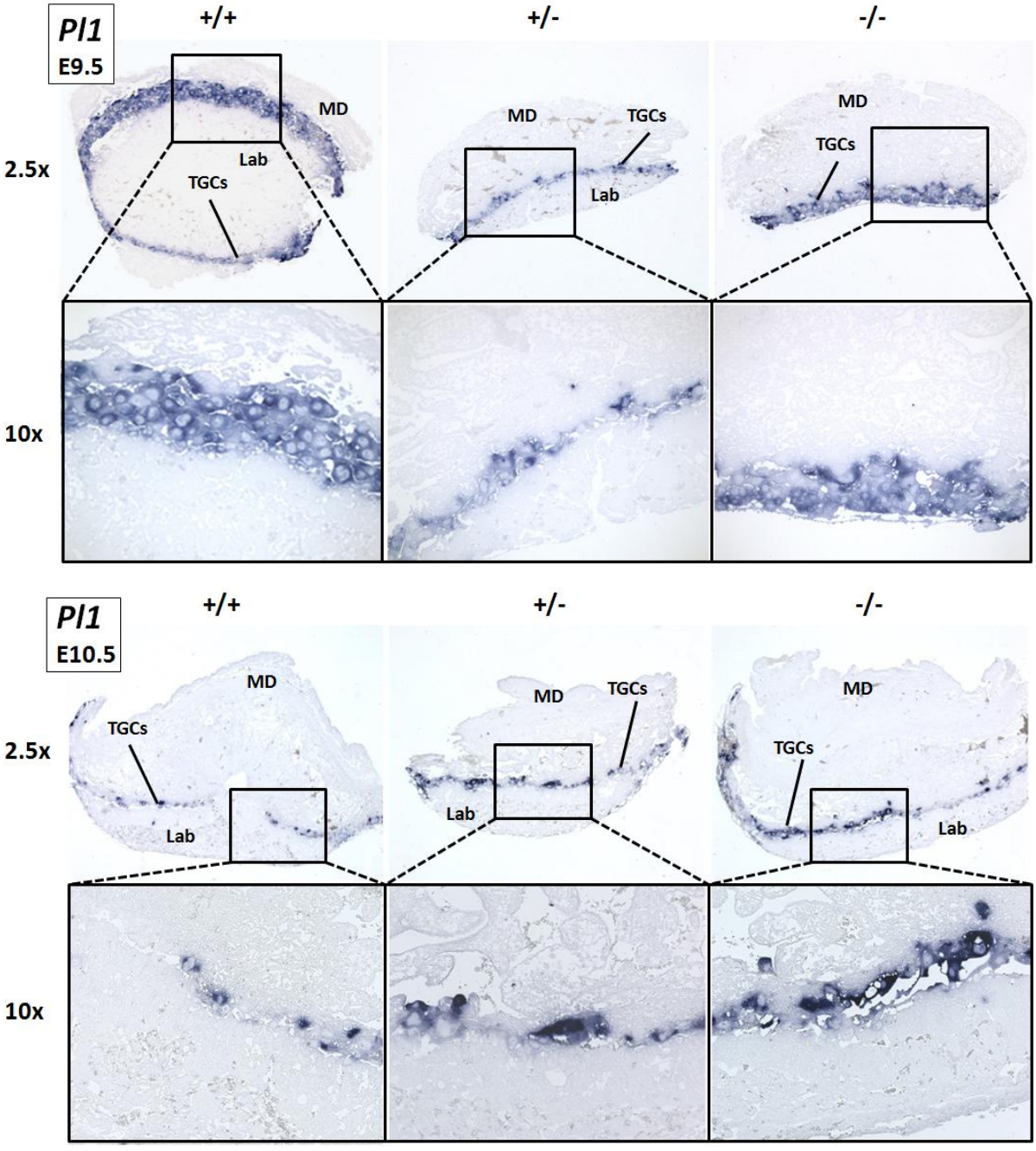

Figure 15: The expression of *Pl1* in *Rnf121* +/+, +/- and -/- placenta
TGCs expressing the *Pl1* are detectable in all three placenta genotypes in both embryonic stages E9.5 and E10.5. By E10.5, the expression of *Pl1* in TGCs decreased in *Rnf121*$^{+/+}$ and *Rnf121*$^{+/-}$ placenta. The magnification was 2.5x and 10x. Lab = Labyrinth, MD = Maternal decidua, TGCs = Trophoblast giant cells.

A third trophoblast marker tested was the *Pcdh12*. This marker was used for detection of glycogen trophoblast cells (GCs) which arise from the ectoplacental cone (EC). From E7.5, the *Pcdh12* expression can be detected in GC precursors within the EC. From E10.5 those cells start to accumulate glycogen and migrate in clusters toward the maternal decidua (Bouillot *et al*., 2006). The expression of *Pcdh12* was examined at E10.5. The clusters of GCs were present in the trophoblast layer of *Rnf121*$^{+/+}$ and *Rnf121*$^{+/-}$ placenta. In contrast, this phenomenon was not observed in *Rnf121*$^{-/-}$ placenta (Fig. 16).

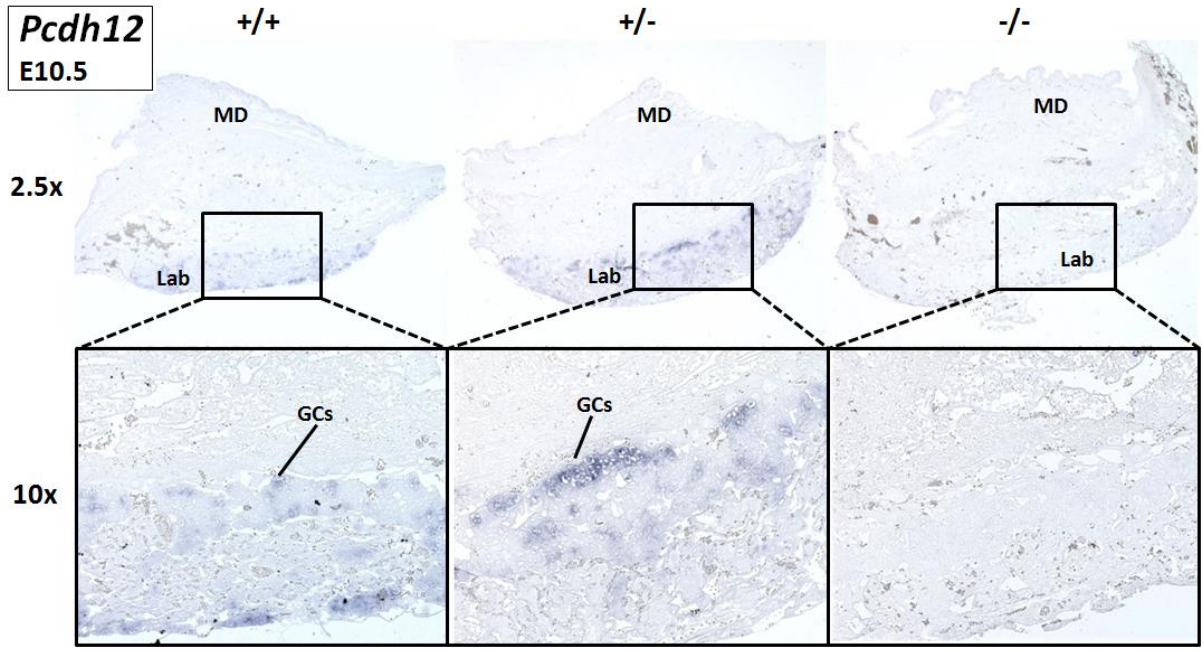

Figure 16: The expression of *Pcdh12* in *Rnf121* +/+, +/- and -/- placenta
In *Rnf121*$^{+/+}$ and *Rnf121*$^{+/-}$ placenta were detected the GC clusters. In *Rnf121*$^{-/-}$ placenta, even a single GC islet was not detected. The magnification was 2.5x and 10x. Lab = Labyrinth, MD = Maternal decidua.

In order to characterize the labyrinth, the expression of *Mest* marker was determined. *Mest* is expressed by fetal endothelial cells surrounding the capillaries within the labyrinth. Its expression is detectable after the chorioallantoic attachment at E8.5 (Screen *et al*., 2008; Katsanou e*t al.*, 2009). By establishment of this gene expression, the vascular development in the placenta can be characterized. Here it is shown that *Mest*-positive cells were detected only in *Rnf121*$^{+/+}$ and *Rnf121*$^{+/-}$ at E9.5 with no evidence in *Rnf121*$^{-/-}$ placenta. At E10.5, the expression was detectable also in *Rnf121*$^{-/-}$ placenta, but the labyrinthine vessels were far less branched than in the placenta of littermates at this stage what points to underdeveloped labyrinth vascularization. Interestingly, the labyrinth of *Rnf121*$^{+/-}$ at E10.5 seemed to be smaller than in the case of wt (Fig. 17).

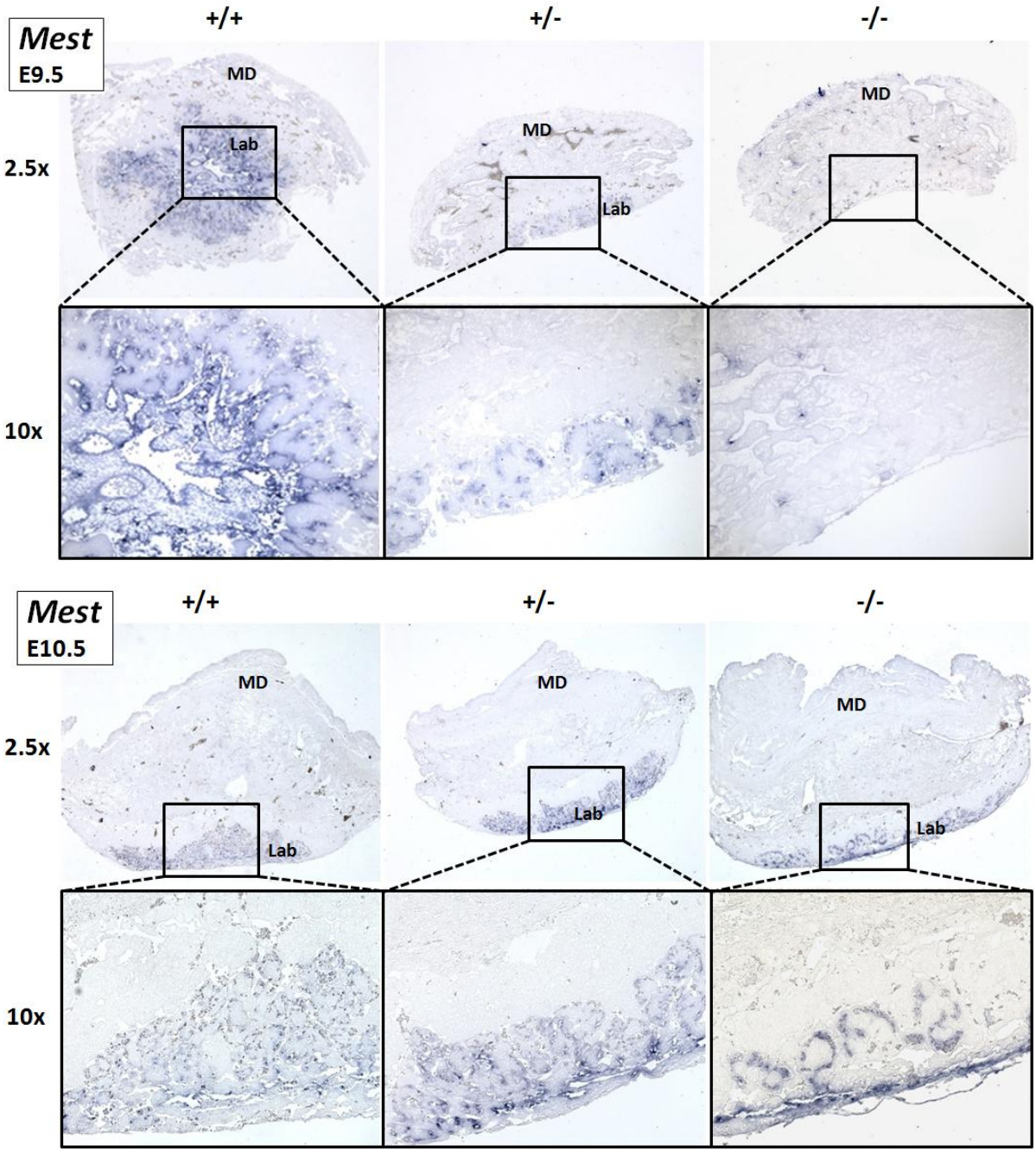

Figure 17: The expression of *Mest* in *RNF121* +/+, +/- and -/- placenta
The labyrinth vascularization in *Rnf121*$^{+/-}$ placenta is underdeveloped. The magnification was 2.5x and 10x. Lab = Labyrinth, MD = Maternal decidua.

5.1.4. Inspection of Hbb-bH1 mRNA expression in yolk sac

Since the localization of the vascular developmental defect is not known, besides the embryo and placenta, the yolk sac was studied as well. For this purpose, the expression of *Hbb-bH1* marker which is characteristic for primitive proerythroblasts – the precursors of fetal erythrocytes (McGrath e*t al*., 2003), was determined. To test expression of this gene, the whole mount *in situ* experiment was performed on E8.5 when primitive proerythroblasts begin to emerge

from blood islands. However, at E8.5, only *Rnf121*$^{+/+}$ and *Rnf121*$^{+/-}$ embryos were successfully dissected as all *Rnf121*$^{-/-}$ embryos were resorbed. As seen on wt structure (Fig. 18), the primitive proerythroblasts should cluster in the shape of a ring, which is around the edge of the yolk sac at this stage. A similar pattern was observed in the yolk sac of *Rnf121*$^{+/-}$ embryo, though the *Hbb-bH1* mRNA expression was higher (Fig. 18). This preliminary experiment has to be repeated to verify the result and compare it with yolk sac structure from *Rnf121*$^{-/-}$ embryo.

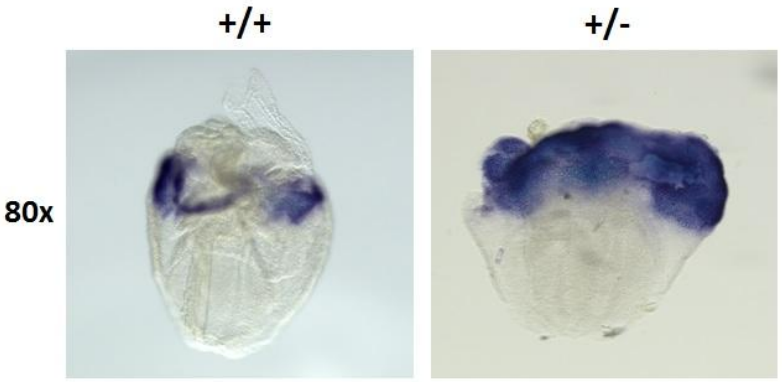

Figure 18: The expression pattern of *Hbb-bH1* in *Rnf121*$^{+/+}$ and *Rnf121*$^{+/-}$ yolk sac
The *Hbb-bH1* is expressed by primitive proerythroblasts of blood islands, which at E8.5 form a ring around the edge of the yolk sac. This phenomenon is detectable in both genotypes with a higher expression in the *Rnf121*$^{+/-}$ yolk sac.

5.2. Murine Rnf121 participates in the activation of the NF-κB pathway

In 2014, RNF121 was described to be involved in the activation of NF-κB pathway (Zemirli *et al*., 2014). In the *RNF121*-silenced HEK293T cells, the degradation of the IκBα was hampered and the transcription factor dimer p65/p50 levels in nuclear fraction were reduced. However, the RNF121 did not ubiquitinate the IκBα directly. We were wondering whether this phenomenon can be observed in our mouse model. For this purpose, the ability of induction of NF-κB signaling pathway in MEF cells by inspection of p65 subcellular localization was tested upon TNF-α treatment.

In non-induced MEF cells, the p65 subunits were present mostly in the cytoplasm (Fig. 19). After TNF-α induction, the p65s in wt MEFs were transported into the nucleus, whereas in majority population of the *Rnf121*$^{-/-}$ MEFs, most of p65s still remained in the cytoplasm.

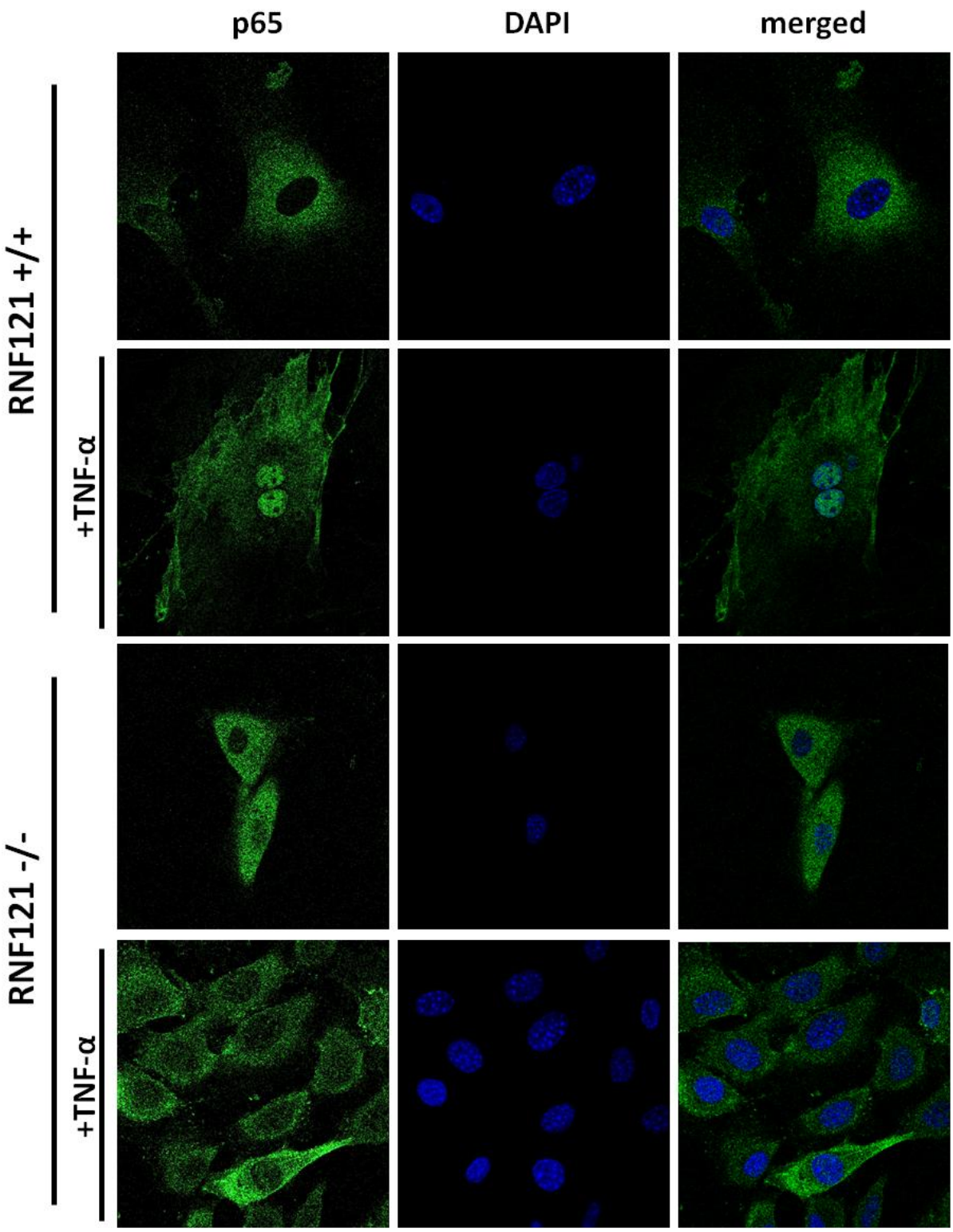

Figure 19: RNF121 regulates translocation of NF-κB transcription factors into the nucleus
Cells were induced with TNF-α for 1 h and stained with anti-p65 primary antibody. In majority population of *Rnf121*$^{-/-}$ MEFs, the translocation of p65 into the nucleus did not occur after the TNF-α induction.

5.3. Searching for the RNF121 interacting partners/substrates

Identification of interacting partners/substrates is necessary for better understanding of the protein function. In the case of RNF121, establishment of interacting partners or substrates is fundamental for better explanation of its function not only in the NF-κB pathway and other signaling pathways but also in other processes including membrane trafficking.

5.3.1. Generation of pCMV6-HsRNF121-myc-FLAG vector

In order to identify the interacting partners or substrates for RNF121, the pull-down approach via FLAG-tag was performed. It was necessary to prepare a vector carrying *Rnf121* in fusion with FLAG tag, through which RNF121 with bound interacting proteins could be precipitated. Hs*RNF121* insert was amplified by PCR from HEK293T cDNA using Phusion polymerase and primers (see Material and methods, Table 2A), through which restriction sites for *Sgf*I and *Mlu*I were generated. *HsRnf186* in *pCMV6*-HsRNF186-myc-TAG, a vector previously constructed in our laboratory by Silvia Petrezsélyová, PhD., was replaced by *HsRNF121*. The vector was restricted with restriction enzymes *Sgf*I and *Mlu*I and two DNA fragments were obtained. A 678 bp fragment corresponding to *HsRNF186* and a 4881 bp fragment corresponded to empty vector (Fig. 20A).

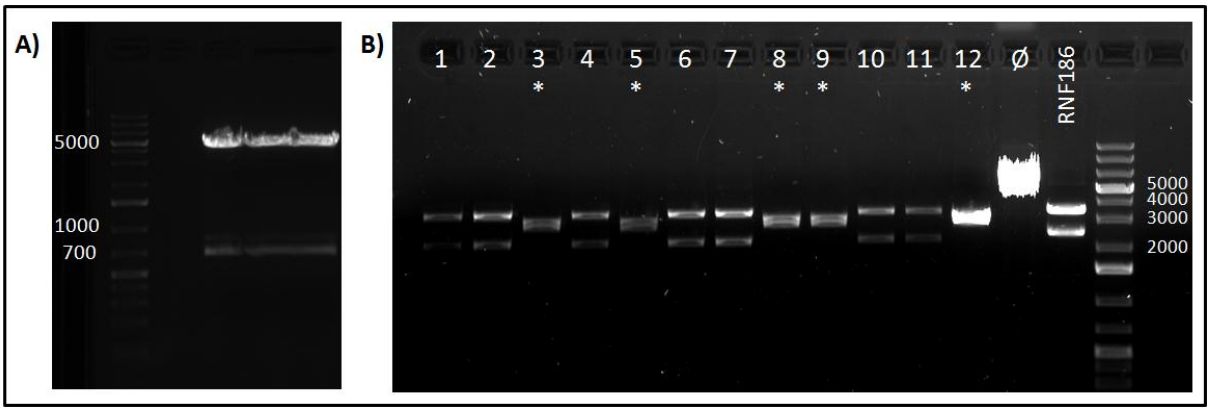

Figure 20: Digested pCMV6-ENTRY-RNF186 vector and restriction analysis of cloning HsRNF121 into pCMV6-ENTRY
A) Picture before gel extraction: the pCMV6-RNF186-myc-FLAG vector was digested with *Sgf*I and *Mlu*I restriction enzymes and loaded on the agarose gel. The 4881 bp fragment corresponding to pCMV6-ENTRY was cut out from the gel, purified and used for further cloning. The 678 bp fragment corresponded to *HsRnf186*.
B) After cloning of *HsRNF121* into pCMV6-ENTRY plasmid, 12 clones were analyzed by restriction digestion with *Stu*I enzyme. Expected size of fragments: pCMV6-HsRNF121-myc-FLAG – 2806 bp and 3056 bp; empty vector - 4919 bp; pCMV6-RNF186-myc-FLAG – 2211 bp and 3348 bp. 5 clones of the total 12 were positive (clones 3, 5, 8, 9, 12). Candidate clones 3 and 5 were sent for sequencing analysis.
Ø = pCMV6-myc-FLAG empty vector; RNF186 = pCMV6-ENTRY-RNF186

The 4881 bp fragment was isolated from the gel, purified and used for the ligation with *HsRNF121*, restricted with the same enzymes to create cohesive ends. XL1 blue competent cells were transformed with ligation mixture and plated onto LB agar plate containing kanamycin. Next day, 12 bacterial colonies were picked up for plasmid DNA isolation and restriction analysis. To determine the size of plasmid DNA, the samples were digested with *Stu*I restriction enzyme (Fig. 20B). 2 candidate clones were sent for sequencing analysis. The prepared vector is shown in the Figure 21.

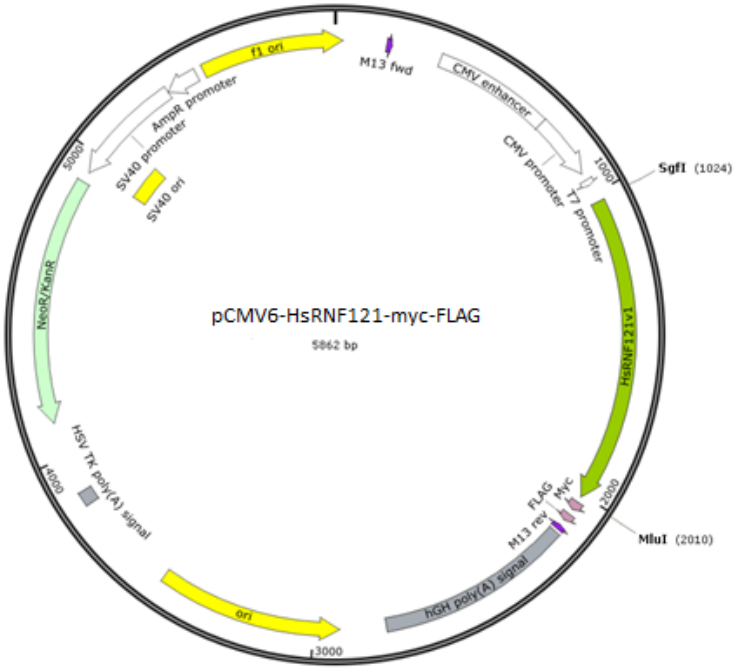

Figure 21: A pCMV6-HsRNF121-myc-FLAG vector map

Restriction enzymes *Sgf*I and *Mlu*I were used for cloning of *HsRNF121* into the vector pCMV6-ENTRY. The vector contains FLAG and myc tag in the fusion with *HsRNF121* and Neomycin/Kanamycin resistance cassette. The final size of the pCMV6-ENTRY-HsRNF121 vector is 5862 bp.

5.3.2. Pull-down of RNF121 interaction partners/substrates

HEK293T cells that reached about 70% of confluency were transfected with pCMV6-HsRNF121-myc-FLAG vector and pCMV6-myc-FLAG empty vector which served as a negative control. For each construct, ten 10-cm plates were used. In parallel, one 10-cm plate was transfected with pCMV6-AC-HsRNF186-GFP, a vector previously constructed in our laboratory by Silvia Petrezsélyová, PhD., to control transfection efficiency of cells. Inspection of these cells by fluorescence microscopy revealed about 70% transfection efficiency (Fig. 22).

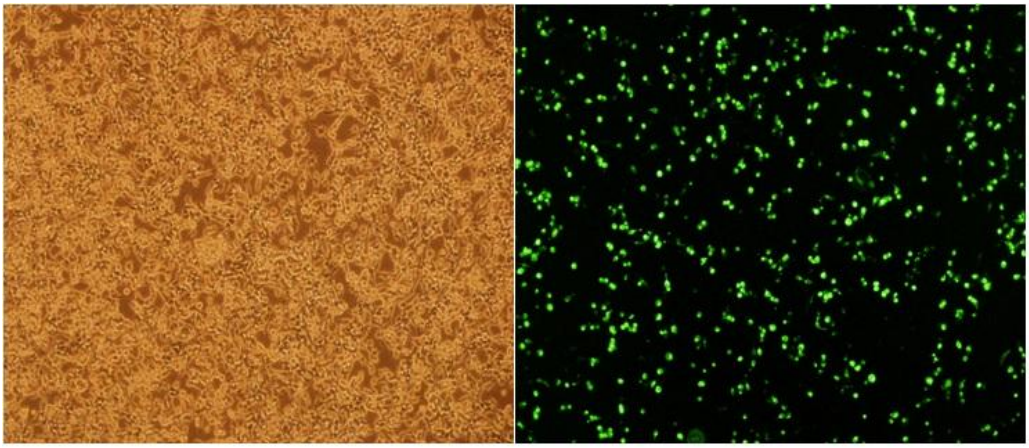

Figure 22: Transfection efficiency of HEK29T cells was around 70%

HEK293T cells transfected with pCMV6-AC-RNF186-GFP served as a control of transfection efficiency.

Cell lysates of cells expressing either pCMV6-HsRNF121-myc-FLAG vector or the corresponding empty backbone vector were prepared by pooling ten plates together in order to obtain large amount of proteins and incubated with anti-FLAG antibody-conjugated agarose beads. To verify that RNF121 was pulled-down and subsequently eluted, the Western blotting method was simultaneously performed (Fig. 23).

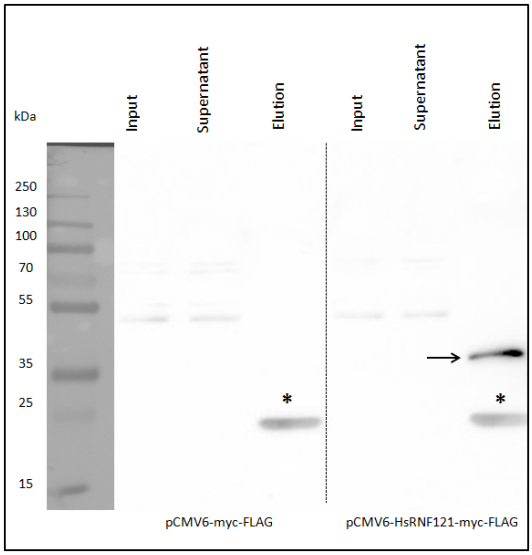

Figure 23: Control of isolation and pull-down of RNF121

The 37 kDa band in the elution of thepCMV6-HsRNF121-myc-FLAG sample lane corresponds to the size of RNF121 (arrow). This band was not detected in the input line. The band of size of 25 kDa corresponds to the light chain of anti-FLAG antibody eluted from the agarose beads (stars).

The band of the size of 37 kDa, which corresponds to RNF121 protein was successfully detected in the elution sample (10% of the total elution was loaded). However, a band of this size was not detected in the input lane (30 µg of total proteins loaded) indicating insufficient isolation of the exogenous RNF121 from the cells. Other unspecific band of the size of 25 kDa was

detected in both, pCMV6-HsRNF121-myc-FLAG and control elution samples. The appearance of these bands is known due to elution of the light chain of the anti-FLAG antibody.

The Coomassie gel analysis was performed for detection of RNF121 immunoprecipitated proteins via anti-FLAG (Fig. 24). By comparison of elution for pCMV6-myc-FLAG vector vs. elution for negative control, we conclude that RNF121 pull down did not work. There were no extra bands corresponding to potential substrates in the pCMV6-HsRNF121 myc-FLAG elution in comparison with the negative control. Ideally, if any extra bands were present, they could be cut off and send for mass spectrometry analysis for their identification.

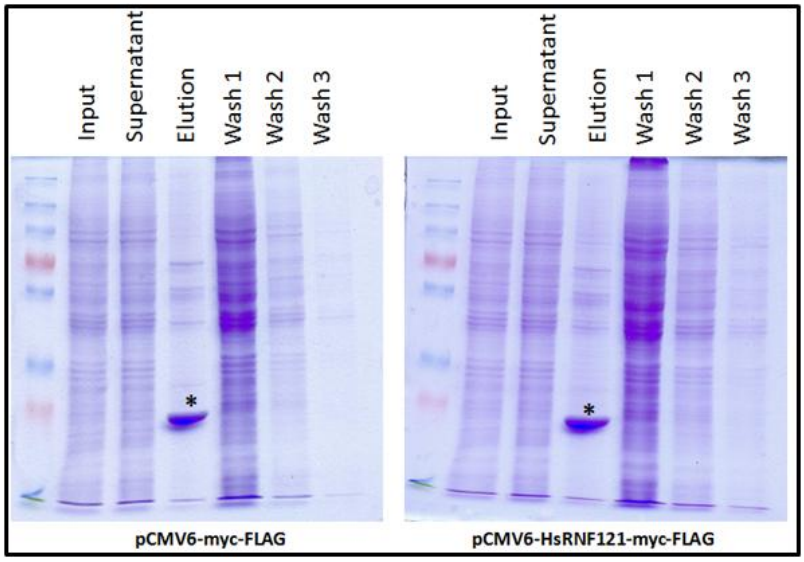

Figure 24: No potential substrates were detected in the pCMV6-HsRNF121 myc-FLAG elution Coomassie gels for pCMV6-HsRNF121-myc-FLAG vector pull-down experiment and the corresponding control are shown.. No extra bands were detected in the elution lane of the pCMV6-HsRNF121-myc-FLAG gel compared to negative control. 25 kDa unspecific bands correspond to light chain of anti-FLAG antibody (stars).

6. Discussion

RNF121 is an evolutionarily conserved RING E3 ubiquitin ligase, which was first described in *C. elegans* as an ER-resident protein having a role in ER stress and distal tip cell migration (Darom e*t al*., 2010; Kovacevic *et al*., 2012). Recent works on RNF121 on mammalian cell lines showed that the protein is localized either in ER or Golgi apparatus and ascribe it different roles at the cellular level. Kallayanee Chawengsaksophak, PhD. (IMG) revealed severe vascular defects in the *Rnf121*$^{-/-}$ embryos (Fig. 7). Most obvious effect was seen on the yolk sac where blood vessels were underdeveloped, very thin and almost undetectable. On null embryos, several haemorrhages were observed. Last but not least, the defects were found also in the placenta, where the vasculogenesis occurred but the vessels seemed to be less developed. Interestingly, RNF121 has been connected with ubiquitination of immature VEGFR-2, thus inhibiting its trafficking from ER to Golgi apparatus what restricts its exposition and signaling on the endothelial cell surface (Maghsoudlou *et al.,* 2015). They described that the overexpression of *RNF121* promoted ubiquitination of VEGFR-2, inhhibited its maturation which resulted in significantly reduced VEGFR-2 presence on the cell surface. In contrast, knockdown of RNF121 resulted in reduced ubiquitination and increased cell surface level of VEGFR-2. However, some of the published results are questionable and are in contrast to the results obtained in our laboratory. For example, the localization of the RNF121, which they described as an ER resident protein, while other works (Zemirli N. *et al*., 2014; Zhao Y. *et al*., 2014) described it as a Golgi localized protein what was also confirmed in our laboratory by using specific antibodies against RNF121 (data not shown). More importantly, we observed the opposite effect of *Rnf121* knockout on mouse embryos, which suffer from underdeveloped vascularization within the yolk sac and placenta and therefore we can expect that lack of the RNF121 led to downregulation of angiogenic signalling.

During embryonic development, the placenta is an essential organ for growth and survival of the fetus, and therefore we decided to focus more on this organ and determine the expression profile of various placental markers. To reach this goal, *in situ* hybridization experiments on placenta sectiones were performed. The RNA probes (*Pcdh12* and *Hbb-bH1*) were successfully prepared via cloning into pGEM-T easy vector and the others (*Hand1, Mest* and *Pl1*) were prepared in our laboratory. The expression of these genes was compared in two different embryonic stages – E9.5 and E10.5. These stages follow the choriallantoic attachment (E8.5) and precede the final establishment of the placenta phenotype.

The results from *in situ* hybridization showed that lack of *Rnf121* leads to formation of smaller trophoblast layer. We observed quite compact and not receding layer of TGCs

in *Rnf121*$^{-/-}$ placenta indicating delayed development of spongiotrophoblast layer. Also, no glycogen trophoblast cells important in later gestation were observed in *Rnf121*$^{-/-}$ placenta. Moreover, the labyrinthine capillaries in null placenta were observed to be clustered and far less developed with restricted branching in comparison with wt and heterozygous littermates (similar phenotype was observed also by *e.g.* Kozak *et* al., 1997; Giroux *et al*., 1999). These results pointed out that the placenta of *Rnf121*$^{-/-}$ embryos is not properly developed with reduced blood vessels, which leads to insufficient nourishment of the fetus. That could explain one of the causes of *Rnf121*$^{-/-}$ embryos dying in midgestation stages. Interestingly, we observed delayed labyrinth development even in the *Rnf121*$^{+/-}$ placenta, which points to phenomenon called small labyrinth – a common placental phenotype described as a consequence of loss of many genes (Watson and Cross, 2000). This is the first observed phenotype for *Rnf121*$^{+/-}$ mice, since they normally survive and do not suffer from any obvious defects.

Further, the possibility that the lack of *Rnf121* could have an impact on hematopoiesis was tested, *i.e*. by determination of *Hbb-bH1* mRNA expression in yolk sac of E8.5 embryos. This stage is characterized with emerging of primitive proerythroblasts from blood islands while forming a ring structure around the edge of the yolk sac. Unfortunately, in the pilot experiment, only *Rnf121*$^{+/+}$ and *Rnf121*$^{+/-}$ embryos at this stage were isolated. Nevertheless, this experiment showed higher *Hbb-bH1* mRNA expression in the case of *Rnf121*$^{+/-}$ embryo. Anyway, to make any conclusions out of this result, it is necessary to repeat the experiment on more litters and especially to establish the *Hbb-bH1* expression in the *Rnf121*$^{-/-}$ embryos. It would be also beneficial to test formation of the vascular network in whole embryo and compare it in all three genotypes, for example with PECAM1 (a marker for endothelial cells) antibody.

One of the functions, already ascribed to RNF121 is the broad regulation of NF-κB activation. This role was described in HEK293T cells by Zemirli and her colleagues (Zemirli e*t al.,* 2014). They reported that the activation is most probably due to the inhibition of IκBα, however, RNF121 did not ubiquitinate IκBα directly. They observed reduced p65/p50 levels in the nucleus after the silencing of *RNF121* expression and also proteasomal degradation of IκBα was hampered. Interestingly, the authors demonstrate that RNF121 colocalizes in the Golgi apparatus with β-TrCP2 and thus they hypothesized that RNF121 could control IκBα degradation through ubiquitination of this protein. In the *in vitro* experiments, we decided to test the participation of RNF121 in the activation of NF-κB pathway on our mouse model. In *Rnf121*$^{-/-}$ MEF cells, we confirmed the inability of p65 to translocate into the nucleus upon the TNF-α induction (Fig. 19).

Within this master thesis, one of the aims was to attempt to identify RNF121 interacting partners or substrates. For this purpose, the pull-down approach via FLAG-tag was performed.

The expression vector pCMV6-HsRNF121-myc-FLAG was constructed and transfected into HEK293T cells. To verify that we are able to pull-down RNF121, the Western blotting method was simultaneously performed. However, there was a problem to detect overexpressed RNF121 in general and we could detect it only in the enriched elution. Because the problem with insufficient isolated exogenous RNF121 occurred repeatedly (data not shown), it indicates that the problem could be in the *RNF121* overexpression itself. The overexpression seems to be toxic for the cells, so the exogenous RNF121 is probably degraded after the transfection. Another possible reason could be the topology of RNF121 as it has up to six transmembrane domains and that might complicate its solubilization from the Golgi membrane. To overcome these problems in future, it will be necessary to work with a low-expression system or to prepare a cell line with endogenously tagged version of *RNF121* prepared by using of CRISPR (Clustered Regularly-Interspaced Short Palindromic Repeats) or TALEN (Transcription Acrivator-like Effector-based Nucleases) approaches.

Based on our results and other works, we could speculate that embryonic lethality of the *Rnf121* mice and related vascularization defects observed in null embryos could be a consequence of missregulation of $SCF^{\beta\text{-}TRCP}$ E3 ubiquitin ligase. As mentioned above, RNF121 indirectly controls proteolysis of a well-known substrate of the $SCF^{\beta\text{-}TRCP}$, IκBα protein. The link between RNF121 and IκBα might be β-TrCP2, a substrate receptor of the $SCF^{\beta\text{-}TRCP}$, that was found to colocalize in the Golgi apparatus (Zemirli e*t al*., 2014). The possibility that ubiquitylation of other components of the $SCF^{\beta\text{-}TRCP}$ by RNF121 cannot be excluded either. In the work of Shaik and his colleagues (2012), it was demonstrated that VEGFR-2, an important angiogenic factor, is a substrate of $SCF^{\beta\text{-}TRCP}$. More recently, another work described VEGFR-2 to be ubiquitylated by RNF121 and thus regulating its fate (Maghsoudlou *et al.,* 2015). Altogether, we believe that RNF121 controls VEGFR-2 via $SCF^{\beta\text{-}TRCP}$ ubiquitylation and therefore, the lack of RNF121 leads to described vascularization defects in $Rnf121^{-/-}$ embryos. This hypothesis has to be further tested in our mouse model.

7. Summary

RNF121 is a RING E3 ubiquitin ligase, of which *in vivo* function in higher eukaryotes have not been described yet. In order to shed light on RNF121 function *in vivo*, *Rnf121* knockout mice (*Rnf121*$^{tm1b(EUCOMM)Hmgu}$) were generated within the International Mice Phenotyping Consortium (IMPC). Repeated heterozygous intercross breedings showed that loss of function of *Rnf121* results in a lethal phenotype and *Rnf121*$^{-/-}$ embryos die prior embryonic day E11.5. Subsequent examination of earlier embryonic stages (E9.5 – E10.5) revealed severe vascular defects in the embryo and in the extraembryonic tissues – placenta and yolk sac. These findings pointed out that RNF121 might have a role in the vascular system development.

The presented thesis aimed to investigate the function of RNF121 in embryonic development in the mouse model. Particular attention was focused on the placenta development. By using of *in situ* hybridization technique, the expression of various placental markers corresponding to different trophoblast layers and endothelial cells in placenta isolated from *Rnf121* mice were characterized. Within the examined stages E9.5 and E10.5, we found out that *Rnf121*$^{-/-}$ embryos suffered from underdeveloped placenta. Obtained results showed thinner and less developed fetal layer, especially the spongiotrophoblasts and less developed vascular branching within the labyrinthine layer. These results are consistent with our hypothesis that RNF121 plays an important role in the vascular development. The whole mount *in situ* hybridization experiment showed a slightly higher expression of *Hbb-bH1* mRNA – a primitive erythroblast marker in the yolk sac of the *Rnf121*$^{+/-}$ embryo comparing to the wt littermate. However, this result must be repeated on a higher number of yolk sacs/embryos from different litters, including *Rnf121*$^{-/-}$ structures.

Further, previous observations of the involvement of RNF121 in the activation of the NF-κB pathway were confirmed on our mouse model. In the *Rnf121*$^{-/-}$ MEF cells, the p65 transcription factor subunits were unable to enter the nucleus upon the TNF-α induction as it normally happens in wt cells.

Identification of substrate specificities of the RNF121 is crucial for understanding of its roles in protein ubiquitination in the regulation of processes, such as vasculogenesis, cell proliferation and apoptosis. Unfortunately, our substrate identification approach was not successful due to inability to purify and pull-down the exogenously expressed RNF121 from the cells. The *RNF121* overexpression seems to be toxic and so it is probably degraded. In future, it will be necessary to use a different approach based on the endogenously expressed *Rnf121* or a low-expression system.

From this perspective, it is possible to look at the RNF121 as an important molecule within the embryonic development, of which absence leads to improper development of the placental trophoblast structures and thus to embryonic death as a result of insufficient nourishment.

8. List of references

Achen, M. G., Gad, J.M., Stacker, S.A., Wilks, A. F. (1997): Placenta growth factor and vascular endothelial growth factor are co-expressed during early embryonic development. *Growth Factors*, 15: 69–80.

Adamson, S. L., Lu, Y., Whiteley, K. J., Holmyard, D., Hemberger, M., Pfarrer, C., Cross, J. C. (2002): Interactions between trophoblast cells and the maternal and fetal circulation in the mouse placenta. *Dev Biol.*, 250(2): 358–373.

Ben-Neriah, Y., Karin, M. (2011): Inflammation meets cancer, with NF-κB as the match marker. *Nat Immunol*, 12(8): 715-723.

Breier, G. (2000): Angiogenesis in Embryonic Development—A Review. *Placenta*, 21: 11-15.

Breier, G., Breviario, F., Caveda, L., Berthier, R., Schnurch, H., Gotsch, U., Vestweber, D., Risau, W., Dejana, E. (1996): Molecular cloning and expression of murine vascular endothelial-cadherin in early stage development of cardiovascular system. *Blood*, 87(2), 630–64.

Brzovic, P. S., Rajagopal, P., Hoyt, D. W., King, M. C., Klevit, R. E. (2001): Structure of a BRCA1-BARD1 heterodimeric RING-RING complex. *Nat Struct Biol.*, 8(10), 833-837.

Carmeliet, P., Ferreira, V., Breier, G., Pollefeyt, S., Kieckens, L., Gertsenstein, M., Fahrig, M., Vandenhoeck, A., Harpal, K., Eberhardt, C., Declercq, C., Pawling, J., Moons, L., Collen, D., Risau, W., Nagy, A. (1996): Abnormal blood vessel development and lethality in embryos lacking a single VEGF allele. *Nature*, 380(6573): 435–439.

Carmeliet, P., Lampugnani. M. G., Moons, L., Breviario, F., Compernolle, V., Bono, F., Balconi, G., Spagnuolo, R., Oostuyse, B., Dewerchin, M., Zanetti, A., Angellilo, A., Mattot, V., Nuyens, D., Lutgens, E., Clotman, F., de Ruiter, M. C., Gittenberger-de Groot, A., Poelmann, R., Lupu, F., Herbert, J. M., Collen, D., Dejana, E. (1999): Targeted deficiency or cytosolic truncation of the VE-cadherin gene in mice impairs VEGF-mediated endothelial survival and angiogenesis. *Cell*, 98(2): 147–157.

Cenciarelli, C., Chiaur, D. S., Guardavaccaro, D., parks, W., Vidal, M., Pagano, M. (1999): Identification of a family of human F-box proteins. *Current Biology*, 9(20), 1177–1179.

Chen, Z. J. (2005): Ubiquitin signaling in the NF-kappaB pathway. *Nat Cell Biol.*, 7, 758-765.

Ciechanover, A., Ben-Saadon, R. (2004): N-terminal ubiquitination: more protein substrates join in. *Trends Cell Biol*, 14(3), 103-106.

Ciechanover, A., Heller, H., Elias, S., Haas, A. L., Hershko, A. (1980): ATP-dependent conjugation of reticulocyte proteins with the polypeptide required for protein degradation. *Proc Natl Acad Sci USA*, 77(3), 1365-1368.

Copp, A. J. (1979): Interaction between inner cell mass and trophectoderm of the mouse blastocyst. II. The fate of the polar trophectoderm. *J Embryol Exp Morphol*, 51, 109-120.

Cross, J. C. (2000): Genetic insights into trophoblast differentiation and placental morphogenesis. *Semin Cell Dev Biol.*, 11(2): 105-113.

Cross, J. C., Simmons, D. G., Watson E. D. (2003): Chorioallantoic morphogenesis and formation of the placental villous tree. *Ann N Y Acad Sci*, 995: 84–93.

Darom, A., Bening-Abu-Shach, U., Broday, L. (2010): RNF-121 is an endoplasmic reticulum-membrane E3 ubiquitin ligase involved in the regulation of beta-integrin. *Mol Biol Cell.*, 21, 1788-1798.

deMello, D. E., Sawyer, D., Galvin, N., Reid, L. M. (1997): Early fetal development of lung vasculature. *Am J Respir Cell Mol Biol.*, 16(5): 568–581.

Deshaies, R. J., Joeazeiro, C. (2009): RING domain E3 ubiquitin ligases. *Annu Rev Biochem.*, 78, 399-434.

Downs, K. M. (1998): The murine allantois. *Curr Top Dev Biol.*, 39: 1-33.

Drake, C. J. (2003): Embryonic and adult vasculogenesis. *Birth Defects Res C Embryo Today: Reviews*, 69(1): 73-82.

Drake, C. J., Fleming, P. A. (2000): Vasculogenesis in the day 6.5 to 9.5 mouse embryo. *Blood*, 95(5): 1671–1679.

Duda, D. M., Scott, D. C., Calabrese, M. F., Zimmerman, E. S., Zheng, N., Schulman, B. A. (2011): Structural regulation of cullin–RING ubiquitin ligase complexes. *Curr Op Struct Biol.*, 21, 257-264.

Dumont, D. J., Fong, G., Puri, M. C., Gradwohl, G., Alitalo, K., Breitman, M. L. (1995): Vascularization of the mouse embryo: a study of flk1, tek, tie, and vascular endothelial growth factor expression during development. *Dev Dyn.*, 203: 80–92.

Dye, B. T., Schulman, B. A. (2007): Structural mechanisms underlying posttranslational modification by ubiquitin-like proteins. *Annu Rev Biophys Biomol Struct*, 36, 131-150.

Fakharzadeh, S. S., Trusko, S. P., George, D. I. (1991): Tumorigenic potential associated with enhanced expression of a gene that is amplified in a mouse tumor cell line. *EMBO J.*, 10, 1565-1569.

Ferrara, N. (2004): Vascular endothelial growth factor: basic science and clinical progress. *Endocr Rev.*, 25(4): 581-611.

Ferrara, N., Carver-Moore, K., Chen, H., Dowd, M., Lu, L., O'Shea, K. S., Powell-Braxton, L., Hillan, K. J., Moore, M. W. (1996): Heterozygous embryonic lethality induced by targeted inactivation of the VEGF gene. *Nature*, 380(6573): 439–442.

Freemont PS, Hanson IM, Trowsdale J. 1991. A novel cysteine-rich sequence motif. *Cell*, 64(3), 483-84.

Frescas, D., Pagano, M. (2008): Deregulated proteolysis by the F-box proteins SKP2 and β-TrCP: tipping the scales of cancer. *Nat Rev Cancer*, 8, 438-449.

Giroux, S., Tremblay, M., Bernard, D., Cardin-Girard, J. F., Aubry, S., Larouche, L., Rousseau, S., Huot, J., Landry, J., Jeannotte, L., Charron, J. (1999): Embryonic death of Mek1-deficient mice reveals a role for this kinase in angiogenesis in the labyrinthine region of the placenta. *Curr Biol.,* 9(7): 369-372.

Guillemot, F., Nagy, A., Auerbach, A., Rossant, J., Joyner, A. L. (1994): Essential role of Mash-2 in extraembryonic development. *Nature*, 371(6495): 333–336.

Hayden, M. S., Ghosh, S. (2012): NF-kB, the first quarter-century: remarkable progress and outstanding questions. *Genes Dev.*, 26, 203-234.

Hershko, A., Ciechanover, A. (1982): Mechanisms of intracellular protein breakdown. *Annu Rev Biochem.,* 51: 335-364.

Hyaden, M. S., Ghosh, S. (2008): Shared principles in NF-kappaB signaling. *Cell*, 132, 344-362.
Jackson, D., Olpert, O. V., Bouck, N., Linzer, D.I. (1994): Stimulation and inhibition of angiogenesis by placental proliferin and proliferin-related protein. *Science,* 266: 1581–1584.

Jackson, P. K., Eldridge, A. G., Freed, E., Furstenthal, L., Hsu, J. Y., Kaiser, B. K., Reimann, J. D. R. (2000): The lore of the RINGs: substrate recognition and catalysis by ubiquitin ligases. *Trends Cell Biol.*, 10: 429-439.

Jin, J., Cardozo, T., Lovering, R. C., Elledge, S. J., Pagano, M., Harper, J. W. (2004): Systematic analysis and nomenclature of mammalian F-box proteins. *Genes Dev.*, 18(21): 2573-2580.

Komander, D. (2009): The emerging complexity of protein ubiquitination. *Biochem Soc Trans.*, 37(5): 937-953.

Kovacevic, I., Ho, R., Cram, E. J. (2012): CCDC-55 is required for larval development and distal tip cell migration in *Caenorhabditis elegans. Mech Dev.,* 128: 548-559.

Kozak, K. R., Abbott, B., Hankinson, O. ARNT-deficient mice and placental differentiation. *Dev Biol.,* 191(2): 297-305.

Krebs, L. T., Xue, Y., Norton, C. R., Shutter, J. R., Maguire, M., Sundberg, J. P., Gallahan, D., Closson, V., Kitajewski, J., Callahan, R., Smith, G. H., Stark, K. L., Gridley, T. (2000): Notch signaling is essential for vascular morphogenesis in mice. *Genes Dev.,* 14(11): 1343–1352.

Kroger, C., Vijayaraj, P., Reuter, U., Windoffer, R., Simmons, D., Heukamp, L., Leube, R., Magin, T. M. (2011): Placental vasculogenesis is regulated by keratin-mediated hyperoxia in murine decidual tissues. *Am J Pathol.,* 178(4):1578-90.

Lindahl, P., Johansson, B. R., Leveen, P., Betsholtz, C. (1997): Pericyte loss and microaneurysm formation in PDGF-B-deficient mice. *Science*, 277(5323): 242–245

Linke, K., Mace, P. D., Smith, C. A., Vaux, D. L., Silke, J. Day, C. L. (2008): Structure of the MDM2/MDMX RING domain heterodimer reveals dimerization is required for their ubiquitylation in *trans. Cell Death Differ.,* 15(5): 841-848.

Maisonpierre, P. C., Suri, C., Jones, P. F., Bartunkova, S., Wiegand, S. J., Radziejewski, C., Compton, D., McClain, J., Aldrich, T. H., Papadopoulos, N., Daly, T. J., Davis, S., Sato, T. N.,

Yancopoulos, G. D. (1997): Angiopoitein-2, a natural antagonist for Tie2 that disrupts in vivo angiogenesis. *Science*, 277(5322): 55–60.

Maltepe, E., Simon, M. C. (1998): Oxygen, genes, and development: An analysis of the role of hypoxic gene regulation during murine vascular development. *J Mol Med.*, 76(6): 391-401.

Matsumoto, K., Yoshitomi, H., Rossant, J., Zaret, K. S. (2001): Liver organogenesis promoted by endothelial cells prior to vascular function. *Science*, 294(5542): 559– 563.

McGrath, K. E., Koniski, a. D., Malik, J., Palis, J. (2003): Circulation is established in a stepwise pattern in the mammalian embryo. *Blood*, 101(5): 1669-1676.

Metzger, M. B., Hristova, V.A., Weissman, A. M. (2012): HECT and RING finger families of E3 ubiquitin ligases at a glance. *J Cell Sci*, 125, 531-537.

Metzger, M. B., Pruneda, J. N., Klevit, R. E., Weissman, A. M. (2014): RING-type E3 ligases: Master manipulators of E2 ubiquitin-conjugating enzymes and ubiquitination. *Biochim Biophys Acta*, 1843(1): 43-60.

Moldovan, M. I., D´andrea, A. D. (2009): How the Fanconi anemia pathway guards the genome. *Annu Rev Genet.*, 43, 223-249.

Monkley, S. J., Delaney, S. J., Pennisi, D. J., Christiansen, J. H., Wainwright, B. J. (1996): Targeted disruption of the Wnt2 gene results in placentation defects. *Development*, 122(11): 3343–3353.

Otsumoto, S., Shimada, T., Cui, C. Y., Nakashima, H., Fujiwara, H., Ko, M. S. (1998): Expression of adrenomedullin, a hypotensive peptide, in the trophoblast giant cells at the embryo implantation site in mouse. *Dev Biol.*, 203: 264–275.

Peppel, K., Zhang, L., Orman, E. S., Hagen P. O., Amalfitano, A., Brian, L., Freedman, N. J. (2005): Activation of vascular smooth muscle cells by TNF and PDGF: overlapping and complementary signal transduction mechanisms. *Cardiovasc Res.*, 65(3): 674 – 682.

Petroski, M. D., Deshaies, R. J. (2005): Function and regulation of Cullin-RING ubiquitin ligases. *Nat Rev Mol Cell Biol.*, 6, 9-20.

Pickart, C. M. (2001): Mechanisms underlying ubiquitination. *Annu Rev Biochem*, 70: 503-533.

Pruneda, J. N., Littlefield, P. J., Soss, S. E., Nordquist, K. A., Chazin, W. J., Brzovic, P. S., Klevit, R. E. (2012): Structure of an E3:E2~Ub complex reveals an allosteric mechanism shared among RING/U-box ligases. *Mol Cell*, 47(6): 933-942.

Read, M. A., Brownell, J. E., Gladysheva, T. B., Hottelet, M., Parent, L. A., Coggins, M. B., Pierce, J. W., Podust, V. N., Luo, R. S., Chau, V., Palombella, V. J. (2000): Nedd8 modification of cul-1 activates SCF(beta(TrCP))-dependent ubiquitination of IkappaBalpha. *Mol Cell Biol.*, 20, 2326-2333.

Risau, W. (1997): Mechanisms of angiogenesis. *Nature*, 386(6626), 671–674.

Robert, B., St. John, P. L., Abrahamson, D. R. (1998): Direct visualization of renal vascular morphogenesis in Flk1 heterozygous mutant mice. *Am J Phys.*, 275: F164–172.

Rossant, J., Cross, J. C. (2001): Placental development: Lessons from mouse mutants. *Nat Rev Gen.,* 2, 538-548.

Rotin, D., Kumar, S. (2009): Physiological functions of the HECT family of ubiquitin ligases. *Nat Rev Mol Cell Biol.,* 10, 398-409.

Ryan, H. E., Lo, J., Johnson, R. S. (1998): HIF-1 alpha is required for solid tumor formation and embryonic vascularization. *EMBO J.,* 17(11): 3005–3015.

Schreiber, A., Stengel, F., Zhang, Z., Enchev, R. I., Kong, E. H., Morris, E. P., Robinson, C. V., da Fonseca, P. C., Barford, D. (2011): Structural basis for the subunit assembly of the anaphase-promoting complex. *Nature*, 470, 227-232.

Scott, I. C., Anson-Cartwright, L., Riley, P., Reda, D., Cross, J. C. (2000): The HAND1 basic helix-loop-helix transcription factor regulates trophoblast differentiation via multiple mechanisms. *Mol Cell Biol.,* 20(2), 530-541.

Screen, M., Dean, W., Cross, J. C., Hemberger, M. (2008): Cathepsin proteases have distinct roles in trophoblast function and vascular remodelling. *Development,* 135(19): 3311-3320.

Sen, R., Baltimore, D. (1986): NF-kB, the first quarter-century: remarkable progress and outstanding questions. *Cell*, 46(5), 705-716.

Senftleben, U., Cao, Y., Xiao, G., Greten, F. R., Krahn, G., Bonizzi, G., Chen, Y., Hu, Y., Fong, A., Sun, S.-C., Karin, M. (2001): Activation by IKKalpha of a second, evolutionary conserved, NF-kappa B signaling pathway. *Science*, 293, 1495-1499.

Shaik, S., Nucera, C., Inuzuka, H., Gao, D., Garnaas, M., Frechette, G., Harris, L., Wan, L., Fukushima, H., Husajn, A., Nose, V., Fadda, G., Sadov, P. M., Goessling, W., North, T., Lawler, J., Wei, W. (2012): SCF□-TRCP suppresses angiogenesis and thyroid cancer cell migration by promoting ubiquitination and destruction of VEGF receptor 2. *J Exp Med.,* 209(7): 1289-1307.

Shalaby, F., Ho, J., Stanford, W. L., Fischer, K. D., Schuh, A. C., Shwartz, L., Bernstein, A., Rossant, J. (1997): A requirement for Flk-1 in primitive and definitive hematopoiesis and vasculogenesis. *Cell,* 89: 981–990.

Shalaby, F., Rossant, J., Yamaguchi, T. P., Gertsenstein, M., Wu, X. F., Breitman, M. L., Schuh, A. C. (1995): Failure of blood-island formation and vasculogenesis in Flk-1-deficient mice. *Nature*, 376(6535): 62-66.

Sharp, D. A., Kratowicz, S. A., Sank, M. J. George, D. L. (1999): Stabilization of the MDM2 oncoprotein by interaction with the structurally related MDMX protein. *J Biol Chem.,* 274(53): 38189-38196.

Shweiki, D., Itin, A., Neufeld, G., Gitay-Goren, H., Keshet, E. (1993): Patterns of expression of vascular endothelial growth factor (VEGF) and VEGF receptors in mice suggest a role in hormonally regulated angiogenesis. *J Clin Invest.,* 91: 2235–2243.

Simmons, D. G., Natale, D. R., Begay, V., Hughes, M., Leutz, A., Cross, J. C. (2008): Early patterning of the chorion leads to the trilaminar trophoblast cell structure in the placental labyrinth. *Development,* 135(12): 2083-1091.

Skaug, B., Jiang, X., Chen, Z. J. (2009): The role of ubiquitin in NF-κB regulatory pathways. *An Rev Biochem.*, 78, 769-96.

Skowyra, D., Craig, K. L., Tyers, M., Elledge, S. J., Harper, J. W. (1997): F-box proteins are receptors that recruit phosphorylates substrates to the SCF ubiquitin-ligase complex. *Cell*, 91(2), 209-219.

Soares, M. J., Muller, H., Orwig, K. E., Peters, T. J., Dai, G. (1998): The uteroplacental prolactin family and pregnancy. *Biology of Reproduction*, 58: 273–284.

Takao, T., asanoma, K., Tsunematsu, R., Kato, K., Wake, N. (2012): The maternally expressed gene *Tssc3* regulates the expression of MASH2 transcription factor in mouse trophoblast stem cells through the AKT-Sp1 signaling pathway. *J Biol Chem*, 287(51): 42685-42694.

Takeda, K., Ho, V. C., Takeda, H., Luan, D. J., Nagy, A., Fong, G. H. (2006): Placental but not heart defects are associated with elevated hypoxia-inducible factor alpha levels in mice lacking prolyl hydroxylase domain protein. *Mol Cell Biol.*, 26(22): 8336-8346.

Threadgill, D. W., Dlugosz, A. A., Hansen, L. A., Tennenbaum, T., Lichti, U., Yee, D., LaMantia, C., Mourton, T., Herrup, K., Harris, R. C. (1995): Targeted disruption of mouse EGF receptor: effect of genetic background on mutant phenotype. *Science*, 269: 230–234.

Verdecia, M. A., Joazeiro, C. A. P., Wells, N. J., Ferrer, J.-L., Bowman, M. E., Hunter, T., Noel, J. P. (2003): Conformational flexibility underlies ubiquitin ligation mediated by the WWP1 HECT domain E3 ligase. *Mol Cell.*, 11(1): 249-259.

Wang, X. W., Wei, W., Wang, W. Q., Zhao, X. Y., Guo, H., Fang, D. C. (2014): RING finger proteins are involved in the progression of Barrett esophagus to esophageal adenocarcinoma: A preliminary study. *Gut Liver*, 8(5): 487-494.

Watson, E. D., Cross, J. C. (2005): Development of structures and transport functions in the mouse placenta. *Physiology*, 20, 180-193.

Welcsh, P. I., King, M. C. (2001): BRCA1 and BRCA2 and the genetics of breast and ovarian cancer. *Hum Mol Genet*, 10(7): 705-713.

Winston, J. T., Koepp, D. M., Zhu, C., Elledge, S. J. Harper, J. W. (1999): A family of mammalian F-box proteins. *Curr Biol.*, 9(20): 1180–1182.

Winston, J. T., Strack, P., Beer-Romero, P., Chu, C. Y., Elledge, S. J., Harper, J. W. (1999): The $SCF^{\beta\text{-}TRCP}$–ubiquitin ligase complex associates specifically with phosphorylated destruction motifs in IκBα and β-catenin and stimulates IκBα ubiquitination in vitro. *Gen Dev.*, 13, 270-283.

Wooding, F. B. P., Flint, A. P. F. (1994): Placentation. *Marshall's Physiology of Reproduction*, 3(4): 233–460.

Xiao, G., Harhaj, E. W., Sun, S. C. (2001): NF-kappaB-inducing kinase regulates the processing of NF-kappaB2 p100. *Mol Cell.*, 7: 401-409.

Xu, X., Weinstein, M., Li, C., Naski, M., Cohen, R. I., Ornitz, D. M., Leder, P., Deng, C. (1998): Fibroblast growth factor receptor 2 (FGFR2)-mediated reciprocal regulation loop between FGF8 and FGF10 is essential for limb induction. *Development*, 125: 753–765.

Zemirli, N., Pourcelot, M., Dogan, N., Vazquez, A., Arnoult, D. (2014): The E3 ubiquitin ligase RNF121 is a positive regulator of NF-κB activation. *Cell Commun Signal.*, 12(72).

Zhao, Y., Hongdu, B., Ma, D., Chen, Y. (2014): Really interesting new gene finger protein 121 is a novel Golgi-localized membrane protein that regulates apoptosis. *Acta Biochim Biophys Sin*, 46, 668-674.